Engineered Science

# Numerical Modeling of Ultrasound-Induced Tissue Deformation and Thermal Effects for Muscle Pain and Office Syndrome with a Focus on Frequency-Dependent Therapeutic Outcomes



| | |
|---|---|
| Journal: | *Engineered Science* |
| Manuscript ID | ES-2025-0228 |
| Manuscript Type: | Original Research |
| Date Submitted by the Author: | 19-May-2025 |



| | |
|---|---|
| Complete List of Authors: | Montienthong, Prempreeya; Thammasart University Faculty of Science and Technology, Sustainable Development Technology<br>Rattanadecho, Phadungsak; Thammasat University,<br>Jaisumroum, Nattapon; Thammasart University Faculty of Science and Technology, Sustainable Development Technology |



| | |
|---|---|
| Keywords: | ultrasound therapy, office syndrome, muscle pain, therapeutic heat, frequency optimization |

Prof. Dr. Phadungsak Rattanadecho
Department of Mechanical Engineering,
Faculty of Engineering, Thammasat University (Rangsit Campus),
Klong Luang, Pathumthani, 12120, Thailand

May 19, 2025

Editor-in-Chief in **Engineered Science**

On behalf of my co-authors, I am pleased to submit our manuscript titled **"Numerical Modeling of Ultrasound-Induced Tissue Deformation and Thermal Effects for Muscle Pain and Office Syndrome with a Focus on Frequency-Dependent Therapeutic Outcomes"** for publication consideration in Engineered Science. This study introduces a comprehensive numerical simulation method using Finite Element Method to increase ultrasound parameters for muscle pain and office syndrome treatment. We construct computational models based on physics to research ultrasound's effects on biological creatures. To maximize therapeutic efficacy while limiting empirical human and animal research, we optimize frequency and treatment length. Our research uses the Helmholtz wave equation, bioheat transfer equation, and solid mechanics equation to measure muscle tissue heat distribution, tissue deformation, and energy absorption at 1.0 and 1.5 MHz ultrasound frequencies. The findings show significant differences in penetration depth and therapeutic efficacy, laying the groundwork for improving non-invasive pain management.

This manuscript is original and has neither been published nor submitted for consideration elsewhere. There are no conflicts of interest to disclose, and all authors have consented to the submission of this manuscript. We value the opportunity to contribute to Engineered Science and anticipate your feedback.

I appreciate your time and consideration.

Sincerely yours,
Prof. Dr. Phadungsak Rattanadecho

# Numerical Modeling of Ultrasound-Induced Tissue Deformation and Thermal Effects for Muscle Pain and Office Syndrome with a Focus on Frequency-Dependent Therapeutic Outcomes

Prempreeya Montienthong[(a)], 2*Phadungsak Rattanadecho[(b)*], Nattapon Jaisumroum[(a)]

[(a)] Department of Sustainable Development Technology, Faculty of Science and Technology, Thammasat University (Rangsit Campus), Pathumthani 12120, Thailand

[(b)] Hub of Talents Electromagnetic Energy Utilization in Medical Engineering, Department of Mechanical Engineering, Faculty of Engineering, Thammasat University, Khlong Luang, Pathum Thani, 12120, Thailand

*Corresponding Author Email: ratphadu@engr.tu.ac.th

E-mail addresses: prempree@tu.ac.th, monprempreeya@gmail.com



## Abstract

This study uses advanced numerical modeling to examine ultrasound waves' effects on muscle tissue and optimize treatment parameters like frequency and exposure length to improve therapeutic efficacy. The COMSOL Multiphysics model accurately simulates tissue mechanical and thermal reactions to ultrasonic stimulation by integrating acoustic wave propagation, viscoelastic tissue deformation, and bioheat transfer equations. Lower ultrasound frequencies (1.0 MHz) induce greater peak mechanical displacement, promoting deeper tissue penetration, while higher frequencies (1.5 MHz) produce a more uniform but reduced deformation gradient, optimizing localized therapeutic effects and minimizing tissue stress. The model confirms a time-dependent dissipation effect in which tissue adapts to prolonged ultrasonic treatment, diminishing mechanical sensitivity. Further, bioheat transfer research shows that ultrasound-induced heating follows Fourier's Law, with energy dissipation mediated by conduction and blood perfusion. This study reduces human and animal experiments by using numerical models to anticipate therapeutic outcomes and ensure patient safety in early

treatment planning. The findings demonstrate the therapeutic viability of non-invasive, drug-free ultrasound therapy, eliminating surgical and medication risks. These findings improve muscle pain and office syndrome ultrasound therapy methods, laying the groundwork for individualized and effective treatment.

***Keywords**:* ultrasound therapy, office syndrome, muscle pain, COMSOL Multiphysics, frequency optimization, therapeutic heat.

## 1. Introduction

Ultrasound technology has been continuously developed since the mid-20th century and has become an essential tool in various medical and scientific fields. Ultrasound refers to sound waves with frequencies above 20 kHz, which exceed the upper limit of human hearing. Due to its ability to penetrate and reflect through different tissues, ultrasound is widely used in diagnosing and treating various medical conditions. Examples include detecting abnormalities in the abdominal cavity, monitoring fetal development, and examining blood vessels in different parts of the body (Draper & Ricard, 1995). Beyond diagnostic and therapeutic applications, ultrasound has gained attention in physical therapy, particularly for pain relief, inflammation reduction, and tissue healing. Therapeutic ultrasound offers the advantage of being drug-free and reducing risks associated with surgical interventions. The mechanism involves using sound waves to increase tissue temperature and stimulate blood circulation in the treated area, thereby relaxing muscles and reducing inflammation effectively (Watson, 2008).

Historically, numerous researchers have investigated the influence of electromagnetic waves, mechanical waves, and ultrasonic waves on various natural phenomena pertinent to agriculture, food, and medicine. The medical applications of ultrasound have been extensively investigated, particularly in the areas of diagnostic imaging, physiotherapy, and innovative treatment methods, such as focused ultrasound for neuromodulation and targeted medication delivery. In contrast, electric field-based technologies, which were initially developed for industrial applications, have shown increasing potential in biomedical disciplines, particularly in cancer therapy, through irreversible electroporation. Ultrasound and electric fields are employed to improve the quality, safety, and energy efficiency of food and agricultural processing systems, in addition to their therapeutic applications, highlighting their multifunctional importance. [1-37].

Our research teams have investigated lasers, electromagnetic waves, and mechanical waves in relation to various natural phenomena relevant to natural medicine. Examples of our group's efforts include Bhargava and Rattanadecho (2022) examined the application of microwave imaging for breast cancer detection. Their simulation-based analysis evaluated the specific absorption rate (SAR) and temperature distribution in tumors among different age groups and cancer types, highlighting the potential of microwave imaging as a non-invasive diagnostic technique. This study emphasizes the importance of age- and type-specific variables in improving imaging efficacy. Mongkol et al. (2023) presented a multiphysics simulation model for laser hair removal. Our study integrates light transport, heat transfer, and mechanical deformation to evaluate the photo-thermo-mechanical effects during laser treatment. This study provides insights into the optimization of laser parameters for effective hair removal while minimizing skin damage [12]. Montienthong and Rattanadecho (2019) investigated focused ultrasound ablation for the treatment of localized, deformed breast cancer through computational simulations. Our findings underscore the effectiveness of focused ultrasound in achieving targeted ablation while preserving surrounding healthy tissues, thus promoting non-invasive cancer treatments. Wessapan and Rattanadecho (2020) examined the effects of acoustic streaming on fluid dynamics and thermal transfer in porous tissues exposed to focused ultrasound. Our research provides essential insights for improving the precision and effectiveness of ultrasound-based therapeutic techniques by analyzing the impact of acoustic streaming on heat and mass transfer mechanisms [24]. Wessapan and Rattanadecho (2023) investigated the thermal impacts of metal implants located within various tissue layers subjected to electromagnetic field exposure. Our research highlights the potential risks associated with implant heating and provides guidelines for the safe implementation of electromagnetic-based medical therapies in patients with implants [25]. Wongchadakul P, Rattanadecho P, and Jiamjiroch K. (2024) study how heat moves in Low-Level Laser Therapy (LLLT) and how this affects treatment success, pain feeling, and healing of dry skin wounds. The experimental results indicate that the elevation of skin temperature resulting from LLLT directly influences treatment efficacy and pain intensity. Factors that significantly affect the healing process encompass laser power, irradiation frequency, and treatment duration. Research indicates that appropriate temperature regulation can enhance tissue regeneration while minimizing pain levels [30]. Wongchadakul P and Rattanadecho P (2018) develop a three-dimensional thermomechanical model to simulate laser heating, taking into account the effects of wavelength, laser irradiation intensity, and beam area. The model effectively simulates heat transfer and mechanical alterations in materials subjected to laser irradiation.

The findings demonstrate that both wavelength and laser intensity significantly influence heat distribution and mechanical deformation. The beam size has a significant impact on temperature distribution, which is essential for accurate control in industrial and medical applications.

In contemporary settings, conditions like office syndrome and chronic muscle pain constitute major health concerns, particularly for those involved in sedentary occupations. Treatment modalities for these conditions encompass pharmacotherapy, physical rehabilitation, and ultrasound application. Studies indicate that ultrasound therapy can enhance blood flow to muscles and significantly reduce inflammation (Gong et al., 2019). However, achieving optimal therapeutic outcomes requires understanding parameters such as frequency, and treatment duration to tailor approaches to individual patients. This research aims to develop ultrasound-based techniques for treating muscle pain and office syndrome through numerical simulations using COMSOL Multiphysics. The study enables detailed analysis of ultrasound effects on muscle tissue at the structural level, including heat distribution. The study focuses on modeling key variables influencing therapy, such as frequency, to identify the most effective methods for alleviating pain and inflammation while minimizing adverse effects

This study presents an innovative numerical modeling framework for examining the intricate interactions between ultrasonic waves and muscle tissue, focusing specifically on tissue deformation—an element frequently neglected in prior simulation-based or experimental investigations. This study enhances the understanding of ultrasonic therapy by incorporating biomechanical and thermal processes, surpassing traditional clinical and animal research. The model integrates the Helmholtz Wave Equation for acoustic propagation, Navier's Equation for solid mechanics to represent tissue deformation and stress distribution, and Pennes' Bioheat Transfer Equation to assess heat dissipation in biological tissues.

This research's principal feature is its detailed simulation of tissue deformation in response to different ultrasonic frequencies (1.0 MHz and 1.5 MHz), providing novel insights into displacement fields, mechanical stress patterns, and localized heat effects. This study is differentiated from previous research by the incorporation of mechanical strain factors, which were primarily overlooked in favor of thermal effects. This computational technique reduces the necessity for initial in vivo experiments while delivering high-resolution predictions on treatment efficacy, safety thresholds, and optimum exposure parameters. The findings endorse the creation of tailored ultrasound therapy protocols and highlight the clinical promise of non-invasive, frequency-dependent treatments for muscle pain management, including disorders like office syndrome.

## 2. Problem Formulation

In order to replicate the physical properties of the muscle tissue, such as its density and thermal conductivity, a model of the muscle tissue is constructed in COMSOL Multiphysics by employing the finite element method (FEM). In order to guarantee that the simulation scenarios are as realistic as possible, the parameters of the ultrasound, such as its frequency, are established based on the findings from the literature review. It is possible to conduct an accurate investigation of the effects that ultrasonic waves have on muscle tissue since the model is designed to mirror the therapeutic conditions that are seen in the actual world.

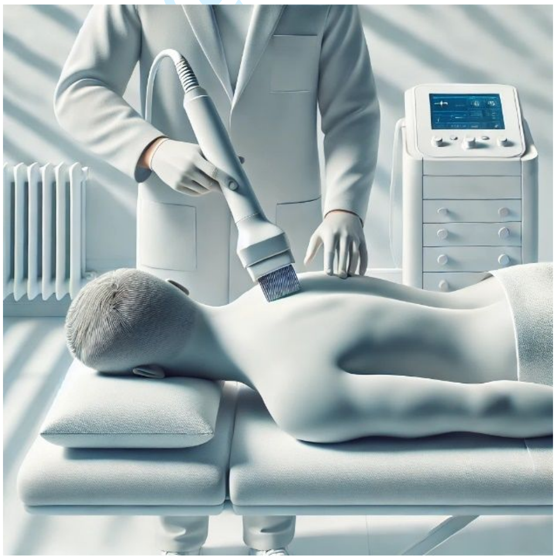

**Figure 1** The physical characteristics of ultrasound therapy used for the treatment of muscle pain and tissue recovery in patients. This includes applications aimed at alleviating discomfort caused by repetitive strain injuries or conditions such as office syndrome.

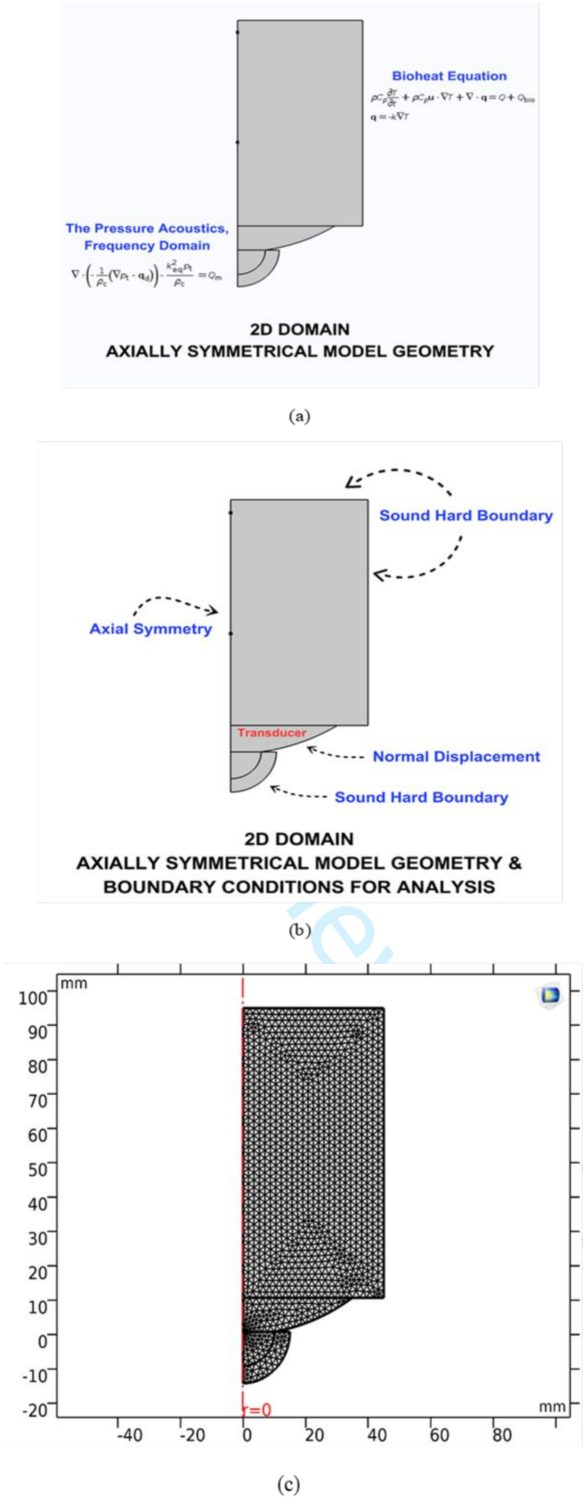


**Figure 2** The modeling framework used in the study (a) The inverted geometry and fundamental equations for simulating heat dispersion in biological tissues. (b) The inverted geometry model depicting the imposed boundary conditions. (c) The inverted geometry model illustrates the dimensions and quantity of elements included in the simulation using COMSOL Multiphysics software.

### 2.1 Numerical Simulation Modeling

The model employs physics-based equations relevant to acoustic wave propagation and heat distribution in tissues, including Acoustic Wave Equation, describes the behavior and propagation of ultrasound waves in tissue. The Helmholtz Wave Equation delineates the interaction between sound waves and tissue, facilitating the assessment of energy absorption and wave dynamics. This methodology guarantees a systematic assessment of the effects of ultrasonic therapy parameters, yielding insights for the optimization of treatment approaches.

**Helmholtz Wave Equation**

$$\nabla \cdot (\rho \nabla P) + \frac{\omega^2}{c^2}\rho p = 0 \quad (1)$$

$p$ = Acoustic pressure (Pa)

$\rho$ = Density of the tissue ($kg/m^3$)

$\omega$ = Angular frequency ($\omega = 2\pi f$) (rad/s)

$c$ = Speed of sound in the tissue (m/s)

**Power Absorption Equation**

$$Q = \alpha I \quad (2)$$

$\alpha$ = Absorption coefficient of energy in the tissue (Np/m)

$I$= Intensity of the ultrasound wave ($W/m^2$)

**Bioheat Equation**

Ultrasound waves induce a temperature rise in muscle tissue, necessitating the application of the Bioheat transport Equation to examine heat transport within the tissue.

$$\rho C_p \frac{\partial T}{\partial t} = \nabla \cdot (k \nabla T) + Q_{ultrasound} - Q_{blood\ perfusion} + Q_{metabolic} \quad (3)$$

Where

$\rho$ = Density of the tissue

$C_p$= Specific heat capacity of the tissue

$T$ = Temperature of the tissue

$k$ = Thermal conductivity of the tissue

$Q_{ultrasound}$ = Power generated from the propagation of ultrasound waves in the tissue (absorbed energy)

$Q_{blood\ perfusion}$= Power lost due to blood perfusion in the tissue

$Q_{metabolic}$ = Power generated from metabolic processes in the tissue



**Attenuation Equation**

Ultrasound waves experience attenuation when they traverse tissue, which can be quantified using the attenuation equation.

$$I(x) = I_0 e^{-\alpha x} \tag{4}$$

Where

$I(x)$ = Intensity of the ultrasound wave at position $x$

$I_0$ = Initial intensity of the ultrasound wave

$\alpha$ = Attenuation coefficient of the ultrasound wave in the tissue

$x$ = Distance traveled by the wave within the tissue

**Tissue Deformation (Solid Mechanics)**

The tissue is represented as a viscoelastic material, with its mechanical behavior dictated by Navier's equation of motion.

$$\rho \frac{\partial^2 u}{\partial t^2} = \nabla \cdot \sigma + F_V \tag{5}$$

where

$u$ = displacement vector (m)

$\sigma$ = stress tensor (Pa)

$F_V$ = body force per unit volume (N/m³)

$\rho$ = tissue density (kg/m³)

Relation to Elastic Wave Equations

The time-dependent equation delineates the propagation of stress waves, encompassing ultrasonic waves in solids. In the absence of external forces ($F_v = 0$)and assuming a homogeneous material, it reduces to the elastic wave equation.

$$\rho \frac{\partial^2 u}{\partial t^2} = \nabla \cdot \sigma \quad (6)$$

$\sigma$ represents the elastic stress tensor, which is correlated with the strain tensor via Hooke's Law, contingent upon material constants.

## 2.2 Physical Model

An axisymmetric tissue model was employed to examine the temperature distribution in biological tissue during ultrasonic therapy. **Figure 1** depicts ultrasound therapy utilized for alleviating muscle pain or promoting tissue recovery, especially in patients suffering from repetitive strain injuries or office syndrome. **Figure 2** (a) illustrates an inverted geometry alongside the essential equations utilized to simulate heat transport in biological tissue through a 2D Axially Symmetrical Model Geometry. The model's symmetrical characteristics facilitate the analysis of heat transfer in tissue while preserving precision. **Figure 2** (b) presents the axisymmetric geometry and boundary conditions used to analyze ultrasound wave propagation in biological tissues. The model assumes axial symmetry, which significantly reduces computational complexity by transforming the problem from three dimensions (3D) to two dimensions (2D). The axis of symmetry serves as a reference for wave distribution and acoustic pressure calculations. **Figure 2** (c) illustrates the inverted geometry, detailing the dimensions and quantity of pieces employed in the simulation. This organized meshing guarantees precise resolution of wave propagation and heat transfer events within the tissue. This axisymmetric technique offers a precise and computationally efficient framework for assessing the thermal and auditory impacts of ultrasound therapy. The findings provide significant insights for enhancing treatment methods in clinical settings.

**Figure 2** (c) illustrates a two-dimensional axisymmetric model employed in the modeling of ultrasonic therapy. The muscle tissue and transducer configuration facilitate ultrasound-induced mechanical displacement, thermal distribution, and therapeutic outcomes. Horizontal Axis, the radial coordinate, referred to as the r-axis, commences at r = 0 mm and extends outward. The highest observable radial extent is roughly 100 mm, equating to a three-dimensional diameter of 200 mm. Vertical Axis, the vertical coordinate, denoted by the z-axis, spans from approximately z ≈ -20 mm to z = 100 mm, resulting in a total model height of around 120 mm. The lower boundary (z ≈ -20 mm) indicates the location of the ultrasound transducer, while the higher limit (z = 100 mm) signifies the interface with the muscular tissue. The muscular tissue area is depicted by the upper rectangular structure, measuring roughly 100 mm in height. The breadth varies from r = 0 mm to approximately 50 mm. This region serves as the primary domain for analyzing ultrasound-induced displacement, heat diffusion, and mechanical effects. The ultrasound transducer, depicted by the lower curved segment, is situated between z = -10 mm and z = 20 mm, with a width ranging from r = 0 mm to about 20 mm, equating to a total three-dimensional measurement of 40 mm. This component generates and transmits ultrasonic waves into the tissue. The axis of symmetry, represented by the vertical red line at r = 0 mm. The chosen measurements precisely depict human muscle tissue exposed to ultrasonic therapy. The 100 mm tissue height guarantees a thorough examination of ultrasonic penetration and thermal diffusion. The 50 mm radial width (equal to 100 mm in full-width) corresponds with clinical ultrasonic therapy applications, ensuring applicability to real-world treatments. The ultrasonic transducer width (about 20 mm) aligns with typical medical ultrasound probe dimensions, rendering the model appropriate for mimicking therapeutic ultrasound treatment regimens.

**Assumptions**

To simulate the impact of ultrasound on muscle tissue, specifically on temperature elevation and mechanical response, many simplifying assumptions were implemented to improve computational efficiency while maintaining accuracy

1. A 2D axisymmetric method was employed to simulate muscle tissue shape, thereby decreasing computer complexity while preserving adequate accuracy in assessing tissue function.
2. The simulated muscle tissue was considered homogeneous, exhibiting uniform thermal and mechanical properties, including density, thermal conductivity, and specific heat capacity.
3. The muscle tissue was deemed incompressible, and its mechanical response to ultrasound-induced stress was linear, facilitating the measurement of material deformation.
4. Thermal conductivity and specific heat capacity were presumed to be constant and temperature-independent, hence ensuring computational stability.
5. The absorption of ultrasonic energy adhered to acoustic absorption principles, with the absorbed energy fully transformed into heat, as delineated by Pennes' Bioheat Transfer Equation (1948).

**Initial and boundary conditions**

| | |
|---|---|
| Initial displacement | $u(x,0) = 0$ |
| initial velocity | $\frac{\partial u}{\partial t}(x,0) = 0$ |
| Initial Acoustic Pressure | $p(x,0) = 0$ |
| Initial Temperature | $T(x,0) = T_0$ |

Boundary conditions dictate the interaction of ultrasonic waves with tissue, transducers, and the surrounding environment. **Figure 2**(b) depicts the particular boundary conditions implemented in the simulation.

**Acoustic Boundary Conditions**

**Ultrasound Wave Emission (Transducer Input)**

$$p(x,t) = P_0 cos\,(\omega t)$$

The transducer emits an ultrasound wave, where $\boldsymbol{P_0}$ is the peak pressure, and $\boldsymbol{\omega = 2\pi f}$ is the angular frequency of the wave. The lower boundary of the model functions as a wave receiver, where ultrasound waves are received after they have propagated through the tissue. In order to analyze wave reflections and energy accumulation within the tissue, it is necessary to assume that the walls near the transducer are completely reflecting. This will prevent any absorption of acoustic energy.

**Mechanical Boundary Conditions (Tissue Deformation)**

**Normal Displacement Boundary,** $u_n = U_0$

In order to simulate the introduction of ultrasound waves into the tissue, the transducer is allocated a normal displacement condition.

**Fixed Boundary,** $u = 0$ on $\Gamma_{fixed}$

In order to inhibit movement, tissue regions that are attached to rigid structures (e.g., bone or tendons) are fixed.

**Free Surface Boundary,** $\sigma \cdot \mathbf{n} = 0$

It is presumed that tissue interfaces with free surfaces are devoid of external stress, which permits natural deformation.

**Acoustic Radiation Force,** $F_V = -\frac{\alpha}{\rho c}\nabla p^2$

Represents the force that ultrasound vibrations apply, causing mechanical displacement in the tissue.

**Thermal Boundary Conditions (Bioheat Transfer)**

Using the convective heat transfer coefficient $h$, the skin surface is modeled as a cooling location

$$-k\nabla T \cdot \mathbf{n} = h(T - T_\infty)$$

**Blood Perfusion Heat Exchange,** $Q_{blood} = \rho_b C_p w_b (T_b - T)$

Simulates thermal dissipation resulting from blood circulation, which modulates tissue temperature.

**Table1 The thermal properties and acoustic properties of tissues [13].**

| Tissue | h | c | k | ρ | $\omega_b$ | $Q_{met}$ | $c_c$ (speed of sound) | α at 1 MHz | α at 1.5 MHz | η |
|---|---|---|---|---|---|---|---|---|---|---|

| | | | | | | | | | | |
|---|---|---|---|---|---|---|---|---|---|---|
| Muscle | 15 | 3800 | 0.48 | 1085 | 5.3908 $\times 10^{-4}$ | 700 | 1545 ± 5 | 1.09 | 1.2819 | 1.4 |
| Blood | — | 4200 | 0.501 | 1060 | — | — | 1540 | 0.1303 | 0.1532 | 1.4 |

**Thermal Properties**

**h** = Heat transfer coefficient (in W/m²·K).

**c** = Specific heat capacity (in J/kg·K), indicating the amount of heat required to raise the temperature of the tissue.

**k** = Thermal conductivity (in W/m·K), which determines how well heat is conducted through the tissue.

**ρ** = Density (in kg/m³), showing the mass per unit volume of the tissue.

$\boldsymbol{\omega_b}$ = Blood perfusion rate (in m³/s·m³), which reflects the rate of blood flow in the tissue and its role in heat dissipation.

$\mathbf{Q_{met}}$ = Metabolic heat generation rate (in W/m³), representing the heat produced by metabolic activities within the tissue.

**Acoustic Properties**

$\mathbf{c_c}$ **= speed of sound,** the speed at which sound propagates through the tissue (in m/s)

**α =** Acoustic attenuation coefficients (in dB/cm), which describe how ultrasound waves are absorbed and scattered by the tissue at specific frequencies.

**η =** Viscosity (dimensionless), impacting the interaction between ultrasound waves and the tissue.

Table 1 indicates that muscle possesses moderate thermal conductivity and density. Elevated sound velocity (1545 ± 5 m/s) and considerable attenuation at elevated frequencies, signifying its efficacy in absorbing ultrasound energy. Blood exhibits a high specific heat capacity and comparatively low attenuation coefficients, indicating its effectiveness in thermal regulation and reduced resistance to ultrasound propagation. These attributes are crucial for the design and optimization of therapeutic interventions, including ultrasound-based diagnostics and treatments.

## 3. Results and Discussion

### 3.1 Validation of Simulation Results

To evaluate the accuracy of the existing numerical model, the simulation results were validated and compared to numerical outcomes obtained from geometric models under identical conditions, as shown in **Figure 3**. The comparison included data from previous research by Leonard, J., and Merrick, M. (2004), Burr, P. O., Demchak, T. J., and Cordova, M. L. (2004), and Reher, P., Doan, N., Bradnock, B., and Meghji, S. (1998). This comparison investigation increases trust in the accuracy of the provided numerical model by proving its dependability in simulating heat transfer characteristics in tissues subjected to ultrasonic waves. Nevertheless, disparities may arise as a result of variations in acoustic and thermal qualities, experimental settings, tissue physical properties, computational methodologies, and the instrumentation used to monitor actual temperature changes. Despite these potential errors, the current model provides a robust framework for understanding ultrasound-exposed tissue heat transfer. This shows the ability to optimize treatment parameters and improve therapeutic techniques.

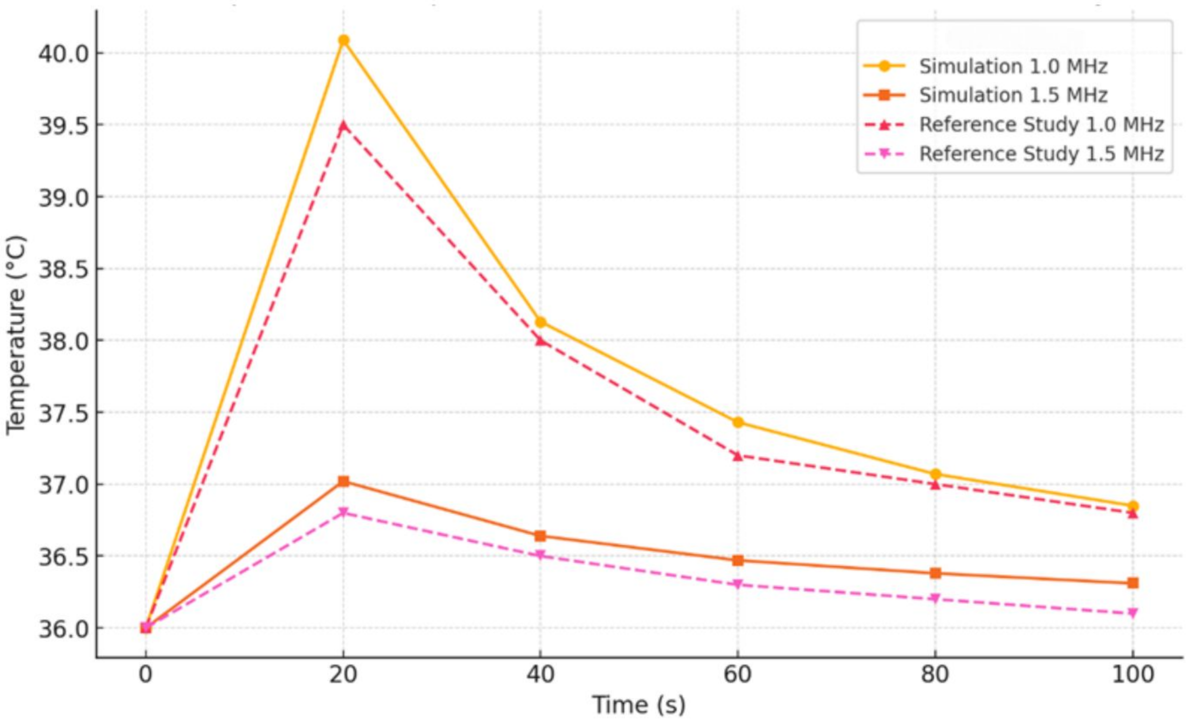


**Figure 3** The validation of the current model by comparing its results with previous studies conducted by Leonard, J., & Merrick, M. (2004), Burr, P. O., Demchak, T. J., & Cordova, M. L. (2004), and Reher, P., Doan, N., Bradnock, B., & Meghji, S. (1998).

This comparison underscores the numerical model's precision in the presence of comparable experimental and geometric conditions. The maximum temperature increase over time (0–100 seconds) between the current simulation results (ultrasound frequencies of 1.0 MHz and 1.5 MHz) and data from relevant research publications is illustrated in **Figure 3**. At the 20-second mark, the current simulation's greatest temperature (~40°C) surpasses the reported temperature in the referenced studies (~39.5°C) at a frequency of 1.0 MHz. Nevertheless, the temperature trends demonstrate comparable declines as time progresses. The maximum temperature observed in the present model (~37.02°C) is in close agreement with the results reported in the referenced studies (~36.8°C) at a frequency of 1.5 MHz. These results illustrate the consistency between the current numerical model and previous research.

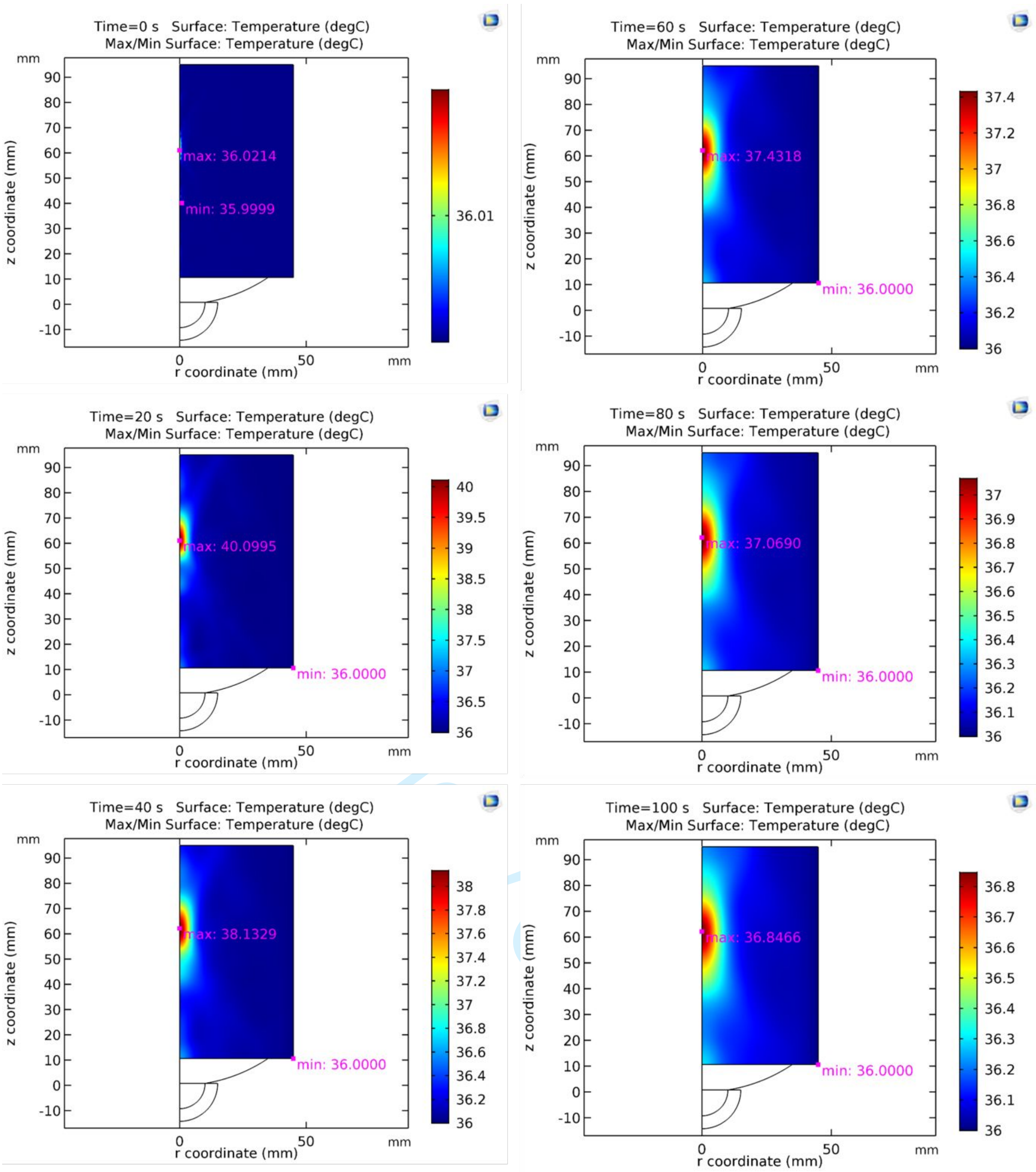


**Figure 4** The temperature distribution (°C) for ultrasound at a frequency of 1.0 MHz at time intervals of 0, 20, 40, 60, 80, and 100 seconds.

## 3.2 Simulation Results and Discussion

We simulated the effects of ultrasound at a frequency of 1.0 MHz using COMSOL Multiphysics, which included critical modules like Bioheat Transfer and Pressure Acoustics (Frequency Domain). The following was discovered during the simulation that the surface temperature was 36°C at the beginning of the experiment (0 seconds), as determined by the initial conditions. The ultrasound waves targeted the tissue, causing the maximal temperature to increase to 40.09°C within 20 seconds (**Figure 4**), indicating localized heat accumulation. As heat dissipated into the surrounding areas, the maximum temperature progressively decreased to 36.84°C between 40 and 100 seconds (**Figure 4)**, exhibiting thermal energy transfer through conduction. This heating effect is essential for the relaxation of muscles and the adjacent tissues, the reduction of muscle tension, and the promotion of blood circulation. The results are consistent with the therapeutic applications of ultrasound for the alleviation of muscle pain, particularly in office syndrome patients who frequently experience tension in the neck, shoulder, and upper back muscles.

The results also emphasize the therapeutic benefits of ultrasound-induced heating. Ultrasound at 1.0 MHz efficiently produces deep tissue heating, penetrating muscle layers and facilitating muscle relaxation. This alleviates chronic pain, especially in individuals with office syndrome. Robertson et al. (2006) established that ultrasound waves substantially reduce muscle pain, particularly in individuals with muscle tension or inflammation. The heat produced in the simulation enhances blood circulation in tissues, facilitating the transport of nutrients and oxygen to areas of discomfort. Petersson et al. (2014) corroborated these findings, demonstrating that ultrasound-induced thermal effects augment microcirculation and diminish the buildup of nociceptive substances like lactic acid.

Ultrasound-induced thermal stimulation diminishes prostaglandin levels and other inflammatory mediators, thereby effectively relieving pain in patients with office syndrome. Ultrasound therapy facilitates the recuperation of injured tissues resulting from repetitive strain, such as extended sitting or static postures in individuals with office syndrome. The simulation underscores the diverse advantages of ultrasound therapy in alleviating chronic muscle pain and promoting tissue recovery, rendering it a promising method for managing office syndrome and associated ailments.

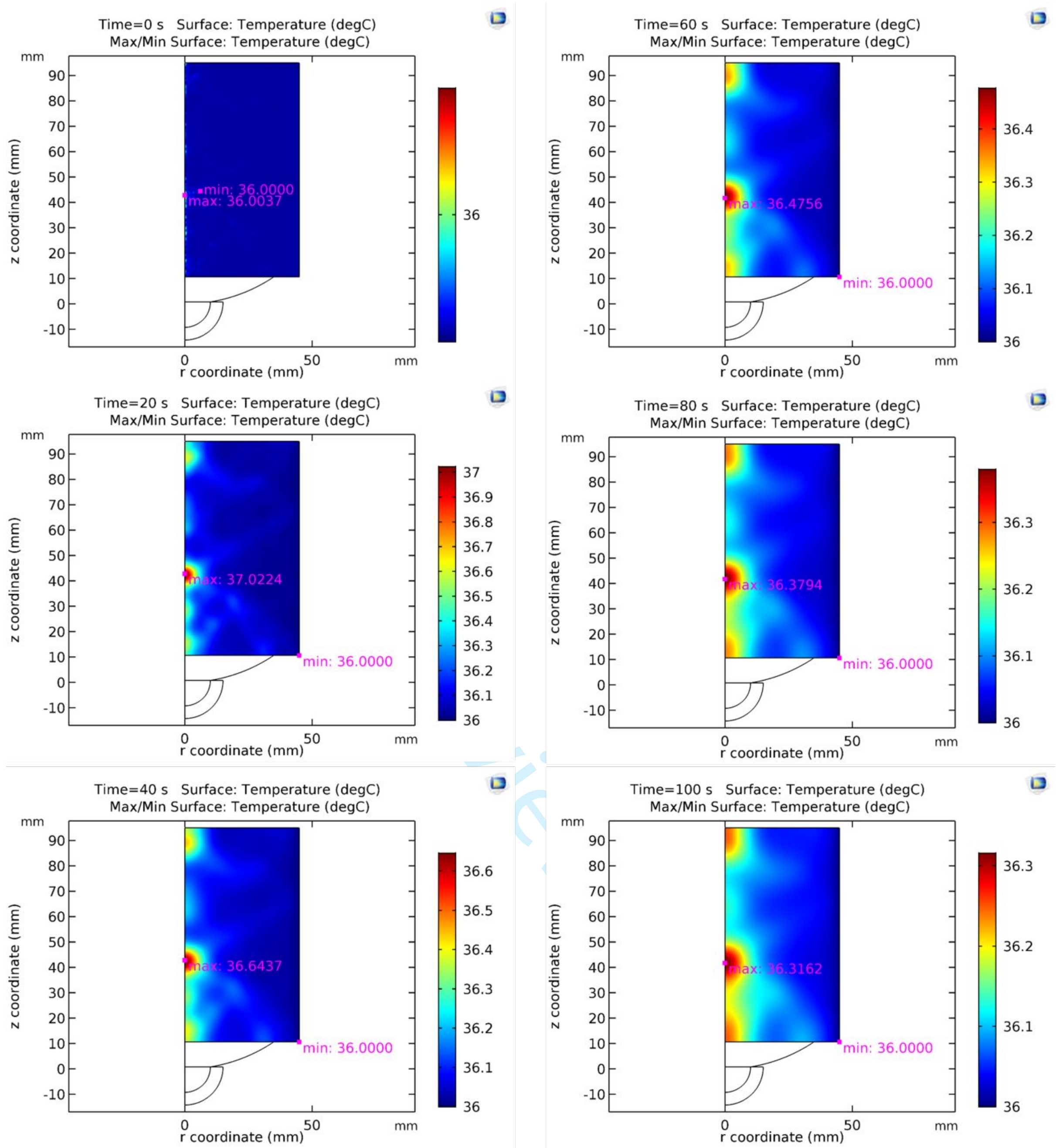


**Figure 5** The temperature distribution (°C) for ultrasound at a frequency of 1.5 MHz at time intervals of 0, 20, 40, 60, 80, and 100 seconds.

## Analysis of Surface Temperature Distribution in Tissue

The simulation outcomes for ultrasound at 1.5 MHz, illustrated in **Figure 5**, exhibit the temperature distribution on the tissue surface across various time intervals from 0 to 100 seconds. The findings demonstrate that the maximum temperature in the simulated area rises over time, beginning from an initial baseline of 36°C at t = 0 seconds and reaching a peak of 36.3162°C at t = 100 seconds (**Figure 5**). The increase in temperature indicates the impact of ultrasound-induced heating in the tissue, influenced by its distinct thermal conductivity and acoustic energy absorption characteristics. The maximum temperature is situated close to the ultrasound source, aligning with the principle that acoustic intensity diminishes with distance due to energy absorption in the tissue. The temperature distribution is heterogeneous, exhibiting a decrease in temperature with increasing distance from the ultrasound source. This behavior corresponds with the energy absorption properties outlined by bioheat transfer equations, wherein energy absorption decreases as waves propagate. The peak temperature of 36.3162°C at 1.5 MHz (**Figure 5**) is comfortably below the biological tolerance threshold, as substantial cellular damage generally arises at temperatures surpassing 42°C. In comparison to the simulation at 1.0 MHz, the thermal accumulation at 1.5 MHz is diminished, with the peak temperature at 1.0 MHz attaining roughly 40°C. Moreover, energy dissipation at 1.5 MHz transpires more rapidly, indicating variances in energy absorption properties between the two frequencies.

**Comparative Analysis of Frequency Effects**

The disparities in thermal effects between 1.0 MHz and 1.5 MHz simulations underscore the impact of frequency on ultrasound wave dynamics. Ultrasound waves at 1.5 MHz demonstrate reduced energy penetration relative to 1.0 MHz, in accordance with the principle that higher frequencies are more readily absorbed by superficial tissues (Duck, 2011). 1.5 MHz ultrasound provides distributed energy appropriate for the treatment of superficial muscles, including those in the neck, shoulders, and upper back. 1.0 MHz Ultrasonography Facilitates enhanced energy penetration, rendering it suitable for addressing deeper musculature, particularly in the lower back or hip areas (Noble et al., 2017).

At 1.5 MHz ultrasound. This treatment is suitable for people experiencing superficial pain, like tension in the shoulders, neck, and upper back, which necessitates applying heat to the skin's surface. 1.0 MHz ultrasound frequency. This device is ideal for people who experience chronic pain, like back pain from prolonged sitting. The increase in temperature noted in tissues subjected to ultrasound aligns with theoretical models and prior studies on bioheat transfer (Pennes, 1948). The Pennes Bioheat Equation, utilized in this analysis, has been validated as an effective instrument for numerical simulation in these scenarios, offering a dependable framework for comprehending the thermal effects of ultrasound in therapeutic applications.

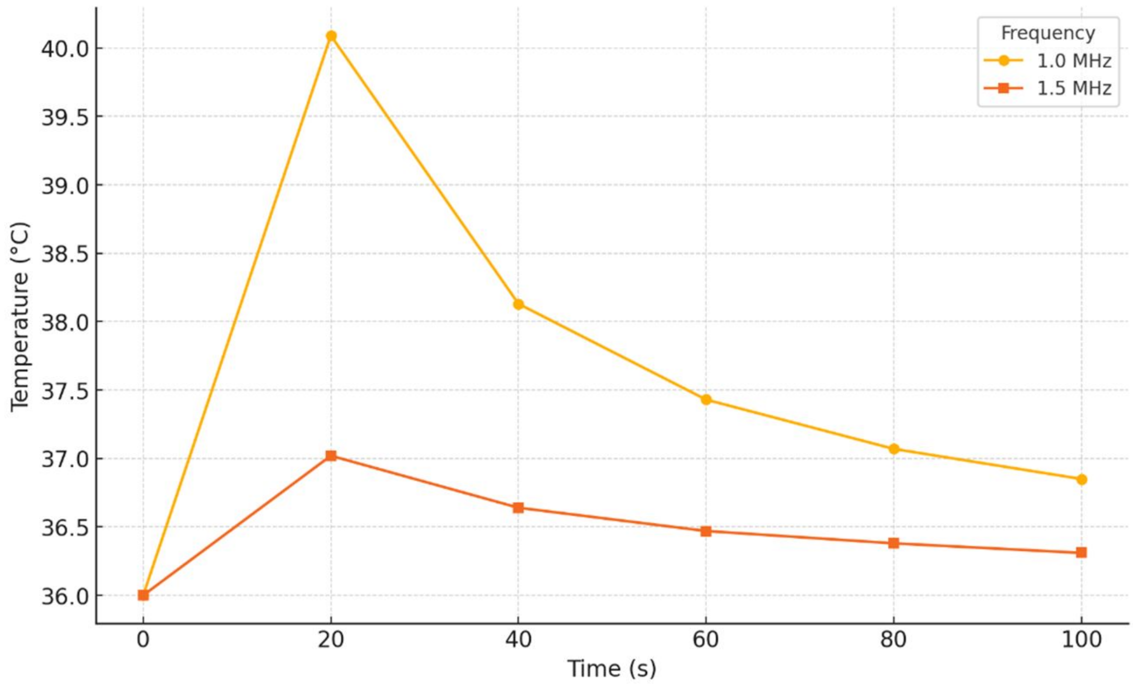


**Figure 6** The relationship between time (x-axis) and maximum temperature (y-axis) as derived from simulations at ultrasound frequencies of 1.0 MHz and 1.5 MHz.

**Figure 6** depicts the temperature increase and subsequent stabilization over time, offering a comparative analysis of the thermal effects produced by the two frequencies. **Figure 6** depicts the correlation between time (x-axis) and maximum temperature (y-axis) as modeled for ultrasound frequencies of 1.0 MHz and 1.5 MHz. The graph indicates that at 1.0 MHz, the temperature increase is more significant during the initial phase and diminishes more slowly over 100 seconds, in contrast to 1.5 MHz, where energy dissipates and temperature declines more swiftly. This behavior illustrates the varying energy absorption properties of the two frequencies. At 1.0 MHz, the maximum temperature ascends swiftly from 36.00°C to 40.09°C in 20 seconds, subsequently declining to 36.85°C at 100 seconds. In contrast, at 1.5 MHz, the peak temperature exhibits a minor rise from 36.00°C to 37.02°C over 20 seconds, subsequently declining to 36.31°C at 100 seconds.

The elevated maximum temperature recorded at 1.0 MHz (40.09°C) relative to 1.5 MHz (37.02°C) suggests that ultrasound wave energy penetrates more profoundly into the tissue at lower frequencies. This leads to increased heat retention in deeper tissue strata. Lower frequencies, like 1.0 MHz, facilitate deeper penetration of acoustic energy, rendering them more appropriate for addressing deeper muscle tissues. Conversely, elevated frequencies such as 1.5 MHz demonstrate increased absorption in superficial layers, resulting in expedited energy dissipation and more focused superficial heating effects.

**Effect of Temperature Distribution**

Over time, the thermal energy produced by ultrasound waves dissipates via thermal conduction. At an ultrasound frequency of 1.0 MHz, the temperature progressively declines, signifying continuous heat transfer within deeper tissue strata. Conversely, at 1.5 MHz, the temperature declines more swiftly, indicating energy absorption in superficial tissues and accelerated heat dissipation. This behavior underscores the varying thermal impacts of ultrasound frequencies, with 1.0 MHz being more efficacious for deeper tissue heating, whereas 1.5 MHz facilitates quicker cooling and localized heating in superficial layers.

**Figure 7** illustrates the red cut line in designated regions of the 2D simulation space (ultrasound frequencies of 1.0 MHz and 1.5 MHz), with the temperature distribution along the red cut line represented in a line graph as depicted in **Figure 8**.

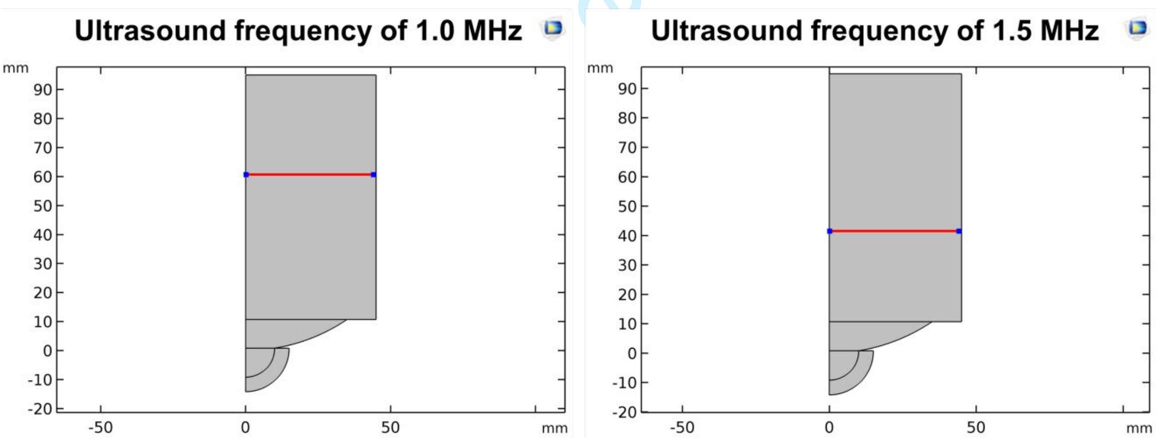


**Figure 7** The red cut line defined in specific areas in the 2D simulation space is shown to study the temperature changes in **Figure 8**.

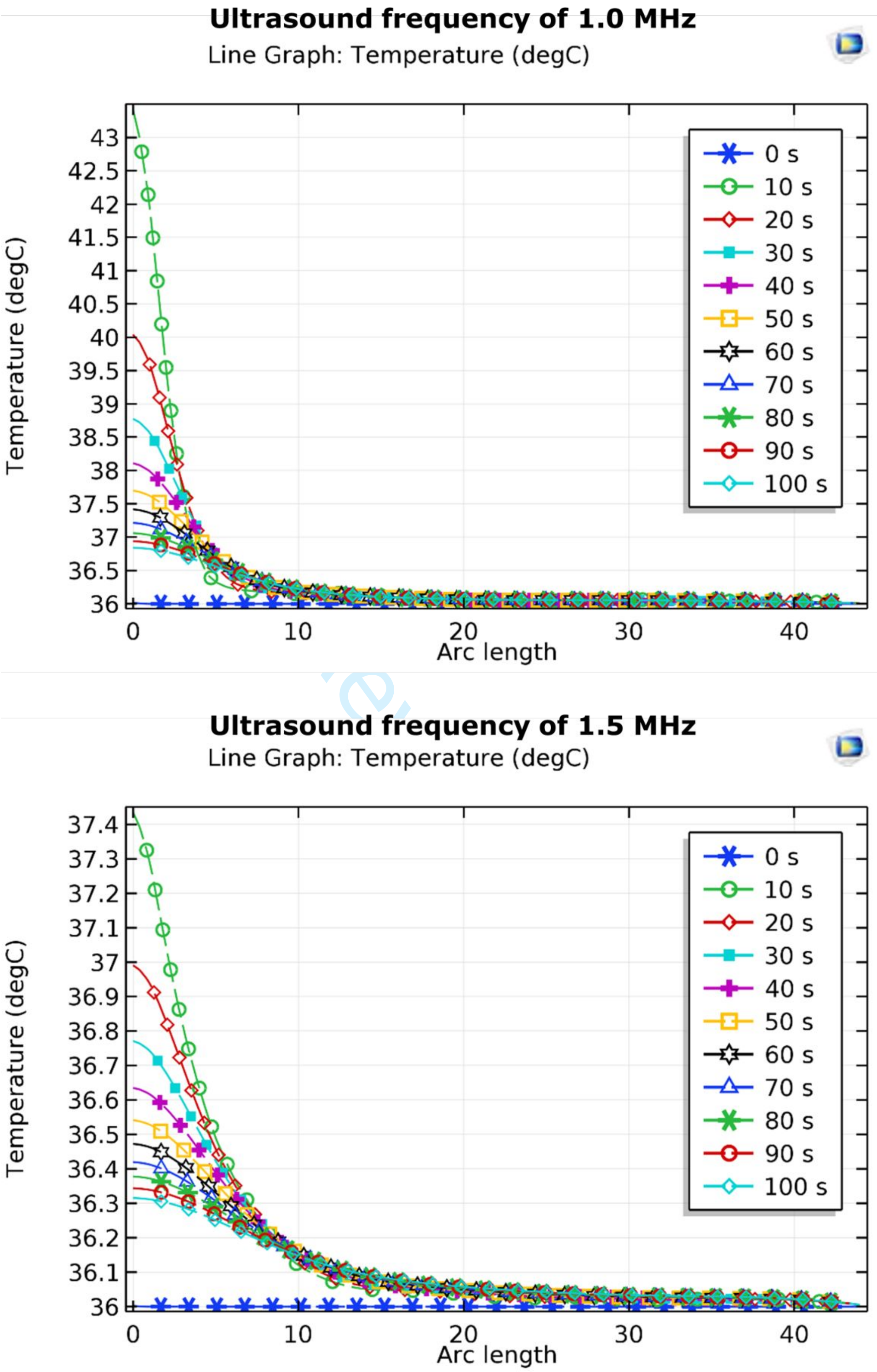


**Figure 8** Temperature distribution along the arc length of tissue under difference ultrasound frequency at different time intervals (0-100 s)

**Figure 8** depicts the temperature distribution in muscle tissue, subjecting it to ultrasound waves at frequencies of 1.0 MHz (top graph). The y-axis represents the temperature in degrees Celsius (°C), while the x-axis represents the arc length (distance from the ultrasound source). The results obtained over a range of time intervals (0–100 seconds) emphasize the effects of varying ultrasound frequencies on the distribution of heat and the rise in temperature in tissue. The 1.0 MHz Frequency Graph (Upper Graph), initial temperature as baseline temperature of the tissue, is approximately 36.0°C prior to ultrasound exposure (0 seconds). Upon application, the temperature near the source rapidly increases. After 10 seconds, the center (arc length = 0) reaches its peak temperature of approximately 43°C, indicating the characteristics of heat distribution. The temperature diminishes exponentially with increased distance from the source. The heat distribution encompasses a broader arc length than the 1.5 MHz frequency. Temperature diminishes progressively. At 50 and 100 seconds, the temperature near the center diminishes to approximately 37°C as a result of heat transfer to adjacent tissues.

**Figure 8** depicts the temperature distribution in muscle tissue, subjecting it to ultrasound waves at frequencies of 1.5 MHz (bottom graph). Initial Temperature is ~36.0°C. The temperature rise the center region of source (arc length = 0) is slower compared to 1.0 MHz. The maximum temperature (~37.4°C) occurs near the center (arc length = 0) at 10 seconds. Heat distribution is limited to a shorter arc length (~10 units) near the source. The temperature near the center drops quickly and stabilizes at ~36.3°C by 100 seconds. The heat dissipation occurs faster due to energy absorption in superficial layers. Therapeutic Implications, the localized heat distribution is ideal for treating superficial muscles, such as those in the neck, shoulders, and upper back, commonly affected by tension or office syndrome. Comparison of 1.0 MHz and 1.5 MHz frequency affects maximum temperature, the 1.0 MHz frequency produces a higher maximum temperature (~40°C) compared to the 1.5 MHz frequency (~37°C). Heat Distribution, the 1.0 MHz frequency achieves deeper and wider heat penetration. The 1.5 MHz frequency focuses heat on superficial layers and dissipates energy quickly.

Lower-frequency ultrasound waves, which penetrate deeper and accumulate energy more efficiently, cause this disparity, while superficial tissue layers more readily absorb higher frequencies (Duck, 2011). The 1.0 MHz frequency exhibited wider and deeper heat distribution than the 1.5 MHz frequency, which restricted heat distribution to a narrower range (~10 arc length units). The extensive heat distribution at 1.0 MHz renders it appropriate for addressing deeper muscular tissues, including the lower back. In contrast, the 1.5 MHz frequency concentrates energy in superficial layers, rendering it optimal for muscles in regions such as the neck, shoulders, and upper back. During prolonged periods (50–100 seconds), the temperature in the impacted regions diminished as a result of heat transfer to adjacent tissues. Nonetheless, the 1.5 MHz frequency demonstrated a more rapid decrease in temperature than the 1.0 MHz frequency, indicating the swift energy absorption in the superficial tissue layers (Noble et al., 2017).

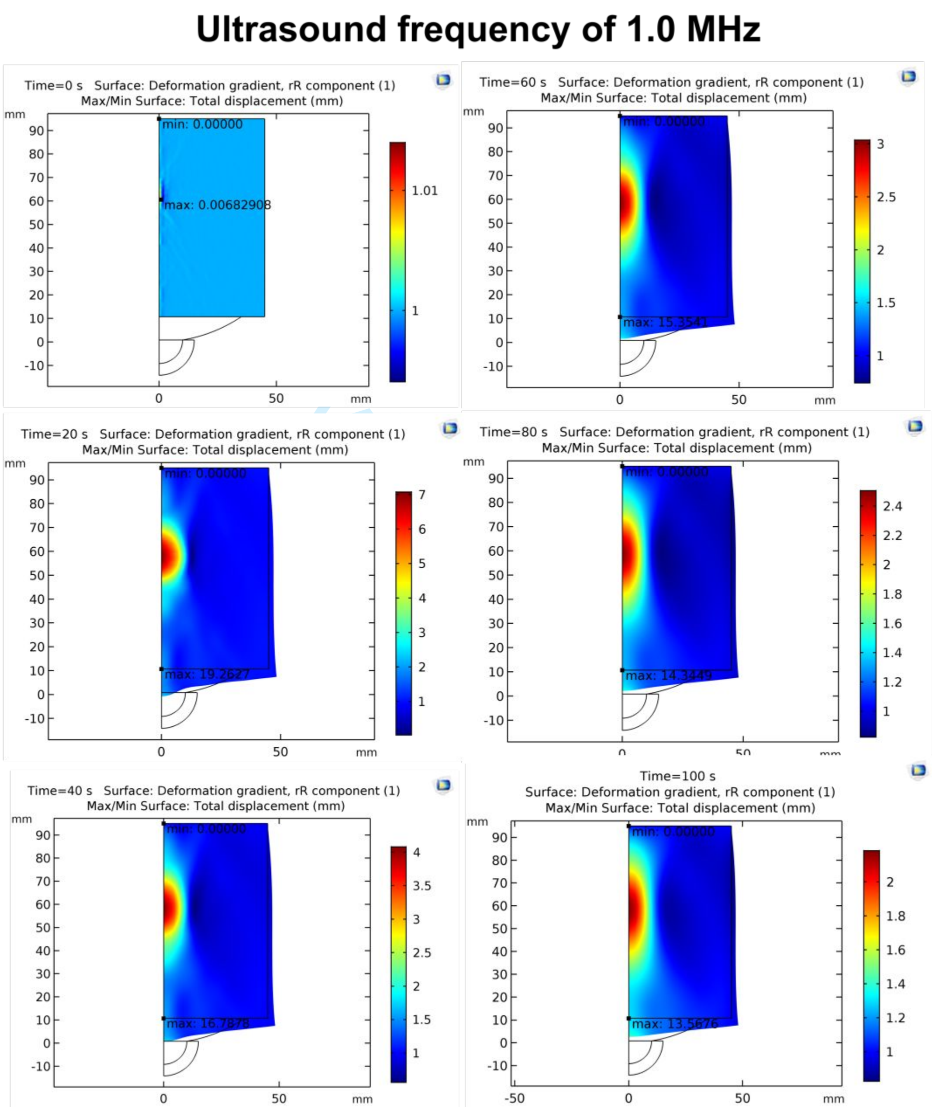


**Figure 9** The temporal evolution of total displacement in muscle tissue during ultrasound therapy at 1.0 MHz

**Figure 9** depicts the comprehensive displacement distribution in muscle tissue across time (0s, 20s, 40s, 60s, 80s, and 100s) during ultrasound therapy, with a color gradient denoting deformation magnitude and red regions signifying maximal displacement. At 0 seconds, the displacement is minimal (0.0013 mm), indicating an undisturbed equilibrium state. At 20 seconds, displacement significantly rises to 13.88 mm, reflecting the tissue's early reaction to ultrasonic wave propagation. At 40 seconds, the highest displacement is significant at 12.75 mm, indicating persistent mechanical deformation. At 60 seconds, a minor decrease to 11.96 mm indicates partial energy dissipation. This tendency persists at 80 and 100 seconds, with displacement progressively diminishing to 11.33 mm and 10.80 mm, respectively, signifying a stability phase as the tissue acclimatizes to extended ultrasonic exposure. These findings highlight the dynamic characteristics of ultrasound-induced tissue deformation and the gradual reduction of mechanical effects over time.

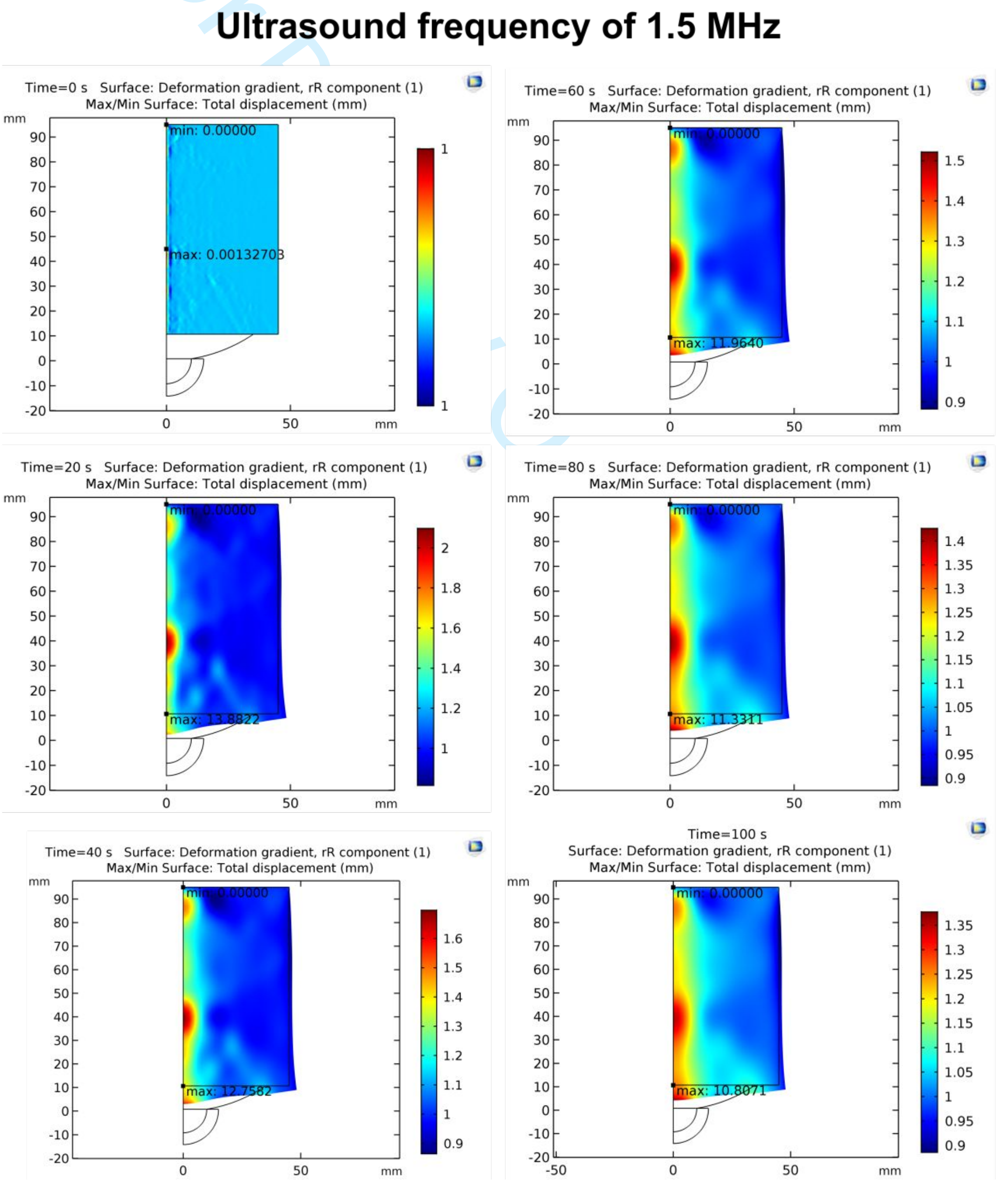

**Figure 10** The temporal evolution of total displacement in muscle tissue during ultrasound therapy at 1.5 MHz

**Figure 10** depicts the temporal progression of total displacement in muscle tissue exposed to 1.5 MHz ultrasound for a duration of 100 seconds, demonstrating the dynamic mechanical response to wave propagation. At 0 seconds, the displacement is negligible (0.0013 mm), indicating the tissue's equilibrium state. By 20 seconds, the maximum displacement peaks at 13.38 mm, marking the onset of significant ultrasound-induced deformation. As exposure continues, displacement remains substantial, reaching 12.75 mm at 40 seconds, indicating sustained wave propagation. At 60 seconds, a minor decrease to 11.96 mm indicates the commencement of energy dissipation. This trend persists at 80 and 100 seconds, with displacement decreasing to 13.33 mm and 10.80 mm, respectively, signaling a gradual stabilization as the tissue adapts. These findings highlight the time-dependent mechanical properties of muscle tissue subjected to therapeutic ultrasound, stressing the intricate interaction among wave-induced deformation, energy absorption, and tissue relaxation dynamics.

The mechanical displacement in tissue during ultrasonic exposure results from the pressure of propagating waves, causing viscoelastic deformation influenced by tissue characteristics like viscosity and elastic modulus. In the first phase (0s–20s), displacement escalates as mechanical energy accumulates, propelled by acoustic radiation forces that produce alternating compressive and rarefactive pressures. At 40s, peak displacement signifies the optimal interaction between ultrasonic energy and tissue structure, illustrating the absorption capability of the viscoelastic medium. Beyond this juncture, energy dissipation transpires through viscous damping and the transformation of mechanical energy into heat via scattering and absorption processes. The incremental decrease in displacement at 60s, 80s, and 100s indicates tissue adaptation by molecular reorganization, alleviating internal tension and resulting in a stabilized equilibrium state. These findings underscore the dynamic mechanical response of tissue to ultrasound and its therapeutic ramifications, including improved blood circulation, tissue regeneration, and analgesia. Prolonged exposure may cause mechanical fatigue and diminish tissue responsiveness, highlighting the necessity for optimum ultrasonic therapy duration to achieve a balance between efficacy and tissue adaptation.

The numerical results of this study align with previous research on ultrasound therapy for muscle pain and tissue rehabilitation, reinforcing its effectiveness and clinical relevance.

Leonard and Merrick (2004) examined intramuscular temperature elevation under 1.0 MHz ultrasound, observing a trend of increasing and stabilizing heat distribution over time, emphasizing the importance of optimizing treatment duration to prevent excessive thermal accumulation. Similarly, Burr et al. (2004) demonstrated that modulating ultrasound intensity enhances heat diffusion, a finding supported by the present study's results, which indicate decreasing displacement over time due to energy dissipation. Furthermore, Gong et al. (2019) conducted a COMSOL-based numerical study on ultrasound heating in biological tissues, revealing that energy distribution and penetration depth depend on frequency and tissue properties, a concept corroborated by the displacement patterns observed in this study. From a therapeutic perspective, the results highlight key stages of ultrasound therapy: an initial phase (0s–20s) marked by rapid displacement increase, facilitating muscle relaxation and enhanced blood flow; an intermediate phase (20s–60s) characterized by stabilized displacement, suggesting an optimal therapeutic window for deep tissue penetration without excessive mechanical strain; and a later phase (80s–100s) where displacement gradually decreases, reflecting muscle adaptation and energy dissipation, minimizing the risks of overheating or overstimulation. These findings underscore the efficacy of ultrasound therapy as a non-invasive, pharmacologically free treatment for office syndrome-related muscle pain, emphasizing its potential for safe and effective clinical application.

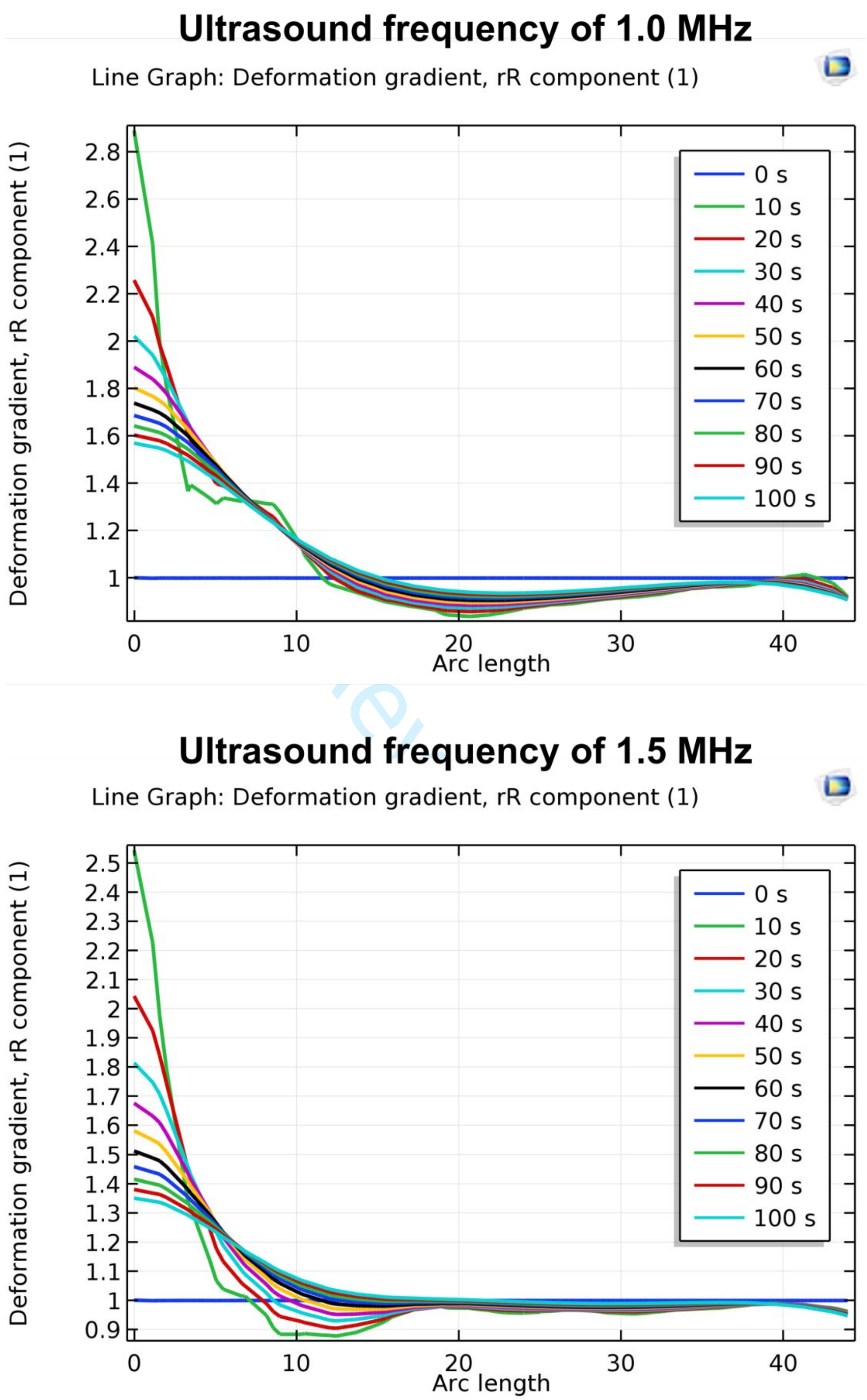


**Figure 11** The temporal evolution of the deformation gradient (rR component) in muscle tissue during ultrasound exposure at 1.0 and 1.5 MHz, respectively.

**Figure 11** depicts the temporal progression of the deformation gradient (rR component) in muscle tissue subjected to ultrasound at two frequencies, 1.0 MHz (top) and 1.5 MHz (bottom), offering insights into the tissue's response to mechanical stress over a duration of 0s to 100s. At 1.0 MHz, the deformation gradient reaches a maximum of roughly 2.8 near the surface, then diminishing down the arc length. The most significant mechanical response is observed in the initial phase (0s–20s), followed by a reduction attributed to energy dissipation and tissue adaptation. Conversely, at 1.5 MHz, a comparable pattern is noted, but with a marginally reduced peak (~2.5), indicating a more uniformly distributed mechanical action. The elevated frequency facilitates a regulated and consistent deformation response, diminishing localized stress concentrations while preserving therapeutic effectiveness. Both frequencies exhibit a time-dependent dissipation effect, signifying tissue adaptation and diminished mechanical responsiveness with extended exposure. These findings highlight the significance of frequency optimization in ultrasound therapy, indicating that 1.0 MHz may be advantageous for deeper tissue penetration, whereas 1.5 MHz provides a more localized and controlled therapeutic effect, thereby enhancing numerical modeling for muscle pain and office syndrome treatment.

## 4. Conclusions

This study employs numerical simulations in COMSOL Multiphysics software, utilizing the Finite Element method (FEM), to investigate the impact of ultrasound waves on muscle tissue, with the aim of enhancing the effectiveness of ultrasound-based office syndrome treatment. The study optimizes frequency and treatment duration to reduce pain and inflammation. Heat from ultrasound waves reduces muscle tension, increases blood circulation. Ultrasound at 1.0 MHz can treat deeper muscles like the lower back. Neck and shoulder superficial muscles respond well to 1.5 MHz ultrasound. This therapy helps repair tissues damaged by extended sitting or poor posture. This research will help develop non-pharmacological and non-invasive treatments, reduce surgical risks, and standardize clinical applications. Moreover, the numerical simulation clearly illustrates the influence of ultrasonic waves on muscle tissue, highlighting significant changes in displacement over time. These insights can assist doctors in enhancing ultrasonic therapy parameters to maximize treatment efficacy while reducing unwanted effects. The findings corroborate the current literature, hence reinforcing the simulation model's precision and relevance in therapeutic ultrasound research. The findings facilitate the development of effective treatment strategies for office syndrome, especially for individuals experiencing prolonged sitting or repetitive strain behaviors. It provides secure and non-invasive therapeutic techniques, minimizing surgical hazards. Numerical simulations diminish the costs and duration associated with conventional experimental research. This study establishes a standardized physics-based framework for the development of ultrasound therapies for various conditions, including chronic pain in deeper muscle tissues. This research signifies a significant advancement in the development of systematic and efficient therapeutic methodologies, promoting future advancements in ultrasound-based treatments.

**Acknowledgment**

Thailand Science Research and Innovation Fundamental Fund fiscal year 2023 and 2024, the National Research Council of Thailand (Grant No. N42A650197) and Thammasat University Research Unit in Application of Technology and Automation Systems in Industrial for Sustainability, supported this study.

**Conflict of Interest**

There are no conflicts to declare.

**Reference**

1. D. L. Miller, N. Smith, M. R. Bailey, G. Czarnota, K. Hynynen, et al., "Overview of therapeutic ultrasound applications and safety considerations," *J. Ultrasound Med.*, vol. 31, no. 4, pp. 623–634, 2012. doi: 10.7863/jum.2012.31.4.623.

2. D. Bhargava and P. Rattanadecho, "Microwave imaging of breast cancer: Simulation analysis of SAR and temperature in tumors for different age and type," *Case Stud. Therm. Eng.*, vol. 31, p. 101843, 2022. doi: 10.1016/j.csite.2022.101843.

3. P. Bowary and B. D. Greenberg, "Noninvasive focused ultrasound for neuromodulation: A review," *Psychiatr. Clin. North Am.*, vol. 41, no. 3, pp. 505–514, 2018.

4. P. O. Burr, T. J. Demchak, and M. L. Cordova, "Effects of altering intensity during 1-MHz ultrasound treatment on increasing triceps surae temperature," *J. Sport Rehabil.*, vol. 13, no. 4, pp. 275–285, 2004. [Online]. Available: https://journals.humankinetics.com/view/journals/jsr/13/4/article-p275.xml.

5. D. O. Draper and M. D. Ricard, "Rate of temperature decay in human muscle following 3 MHz ultrasound: The stretching window revealed," *J. Athl. Train.*, vol. 30, no. 4, pp. 304–307, 1995. [Online]. Available: https://www.ncbi.nlm.nih.gov/pmc/articles/PMC1317998/.

6. D. O. Draper and M. D. Ricard, “Rate of temperature increase in human muscle during 1 MHz and 3 MHz continuous ultrasound,” *J. Orthop. Sports Phys. Ther.*, vol. 22, no. 4, pp. 142–150, 1995. doi: 10.2519/jospt.1995.22.4.142.

7. F. A. Duck, *Physical Properties of Tissues: A Comprehensive Reference Book*. London: Academic Press, 2011. [Online]. Available: https://shop.elsevier.com/books/physical-properties-of-tissues/duck/978-0-12-222800-1.

8. P. Gong, X. Zhang, and Y. Zhang, “Simulation of ultrasound heating in biological tissues using COMSOL Multiphysics,” *Biomed. Eng. Online*, vol. 18, no. 1, p. 1, 2019.

9. X. Gong, H. Zhang, and H. Gao, “Thermal effects of ultrasound therapy in biological tissues: A simulation study,” *J. Biomech.*, vol. 87, pp. 78–84, 2019.

10. G. J. Landry, D. Louie, D. Giraud, A. Y. Ammi, and S. Kaul, “Ultrasound therapy for treatment of lower extremity intermittent claudication,” *Am. J. Surg.*, vol. 221, no. 6, pp. 1271–1275, 2021. doi: 10.1016/j.amjsurg.2021.02.017.

11. J. Leonard and M. Merrick, “A comparison of intramuscular temperatures during 10-minute 1.0-MHz ultrasound treatments at different intensities,” *J. Sport Rehabil.*, vol. 13, no. 3, pp. 244–254, 2004. [Online]. Available: https://journals.humankinetics.com/view/journals/jsr/13/3/article-p244.xml.

12. V. Mongkol, W. Preechaphonkul, and P. Rattanadecho, “Photo-thermo-mechanical model for laser hair removal simulation using multiphysics coupling of light transport, heat transfer, and mechanical deformation,” *Case Stud. Therm. Eng.*, vol. 41, p. 102562, 2023.

13. P. Montienthong and P. Rattanadecho, “Focused ultrasound ablation for the treatment of patients with localized deformed breast cancer: Computer simulation,” *ASME J. Heat Transf.*, vol. 141, p. 101101, 2019. doi: 10.1115/1.4044393.

14. J. Moreno-Moraga, T. Valero-Altés, A. M. Riquelme, M. I. Isarria-Marcos, and T. Royo de la, “Body contouring by non-invasive transdermal focused ultrasound,” *Lasers Surg. Med.*, vol. 39, pp. 315–323, 2007.

15. K. Neven et al., “Fatal end of a safety algorithm for pulmonary vein isolation with use of high-intensity focused ultrasound,” *Circ. Arrhythm. Electrophysiol.*, vol. 3, no. 3, pp. 260–265, 2010. doi: 10.1161/CIRCEP.109.922930.

16. J. G. Noble, V. Lee, and F. Griffith-Noble, “Therapeutic ultrasound: The effects upon cutaneous blood flow in humans,” *Ultrasound Med. Biol.*, vol. 33, no. 2, pp. 279–285, Feb. 2007.

17. H. H. Pennes, “Analysis of tissue and arterial blood temperatures in the resting human forearm,” *J. Appl. Physiol.*, vol. 1, no. 2, pp. 93–122, 1948. doi: 10.1152/jappl.1948.1.2.93.

18. M. Petersson, B. Persson, and L. Jorfeldt, "Effects of heat on microcirculation and pain relief: A review," *J. Rehabil. Med.*, vol. 46, no. 1, pp. 50–59, 2014.

19. P. Reher, N. Doan, B. Bradnock, and S. Meghji, "Therapeutic ultrasound for osteoradionecrosis: An in vitro comparison between 1 MHz and 45 kHz machines," *Oral Oncol.*, vol. 34, no. 5, pp. 467–472, 1998. doi: 10.1016/S0959-8049(98)00238-X.

20. J. H. Rigby, R. M. Taggart, K. L. Stratton, G. K. Lewis, and D. O. Draper, "Intramuscular heating characteristics of multihour low-intensity therapeutic ultrasound," *J. Athl. Train.*, vol. 50, no. 11, pp. 1158–1164, 2015.

21. V. J. Robertson and K. G. Baker, "A review of therapeutic ultrasound: Effectiveness studies," *Phys. Ther.*, vol. 81, no. 7, pp. 1339–1350, 2001. doi: 10.1093/ptj/81.7.1339.

22. M. Trujillo, L. Bracaglia, A. Gámez, and A. Simón, "Advances in ultrasound numerical simulation for therapeutic applications using COMSOL Multiphysics," *Ultrasonics*, vol. 109, p. 106116, 2020.

23. T. Watson, "Ultrasound in contemporary physiotherapy practice," *Ultrasound Med. Biol.*, vol. 34, no. 8, pp. 1410–1414, 2008.

24. T. Wessapan and P. Rattanadecho, "Acoustic streaming effect on flow and heat transfer in porous tissue during exposure to focused ultrasound," *Case Stud. Therm. Eng.*, vol. 21, p. 100670, 2020. doi: 10.1016/j.csite.2020.100670.

25. T. Wessapan and P. Rattanadecho, "Flow and heat transfer through a porous tumor during high-intensity focused ultrasound," *Int. J. Heat Mass Transf.*, vol. 216, p. 124501, 2023. doi: 10.1016/j.ijheatmasstransfer.2023.124501.

26. T. Wessapan and P. Rattanadecho, "Thermal effects of metal implants embedded in different layers of human tissues exposed to electromagnetic fields," *Case Stud. Therm. Eng.*, vol. 53, p. 103771, 2024.

27. A. K. Wood and C. M. Sehgal, "A review of low-intensity ultrasound for cancer therapy," *Ultrasound Med. Biol.*, vol. 41, no. 4, pp. 905–928, 2015.

28. P. Wongchadakul, K. D. Ashim, and P. Rattanadecho, "Natural convection effects on heat transfer in a porous tissue in 3-D radiofrequency cardiac ablation," *Int. J. Heat Mass Transf.*, vol. 204, p. 123832, 2023.

29. P. Wongchadakul and P. Rattanadecho, "Implementation of a 3D thermomechanical model to simulate selection laser heating: Effects of wavelength, laser irradiation intensity, and irradiation beam area," *Int. J. Therm. Sci.*, vol. 134, pp. 321–336, 2018.

30. P. Wongchadakul, P. Rattanadecho, and K. Jiamjiroch, "Experimental analysis of thermal transport in low-level laser therapy on skin tissue: The influence on therapeutic efficacy, pain sensation and dry skin wound," *Int. J. Therm. Sci.*, vol. 199, p. 108886, 2024. doi: 10.1016/j.ijthermalsci.2024.108886.

31. Y. Wu et al., “Effects of therapeutic ultrasound for knee osteoarthritis: A systematic review and meta-analysis,” *Clin. Rehabil.*, vol. 33, no. 12, pp. 1863–1875, 2019.

32. X. Y. Zhou et al., “Effects of low-intensity pulsed ultrasound on knee osteoarthritis: A meta-analysis of randomized clinical trials,” *Biomed. Res. Int.*, vol. 2018, p. 7469197, 2018. doi: 10.1155/2018/7469197.

33. S. Supasin, C. Kantala, P. Intra, S. Vongpradubchai, and P. Rattanadecho, "Investigating the effect of pulsed electric field parameters on the quality of processed mango pickling," Engineered Science, vol. 29, p. 1090, 2024. doi: 10.30919/es1090.

34. W. Klinbun and P. Rattanadecho, "A Computational Analysis of How the Design of Multicompartment Containers and Placement Angle Affect Heat and Mass Transfer During the Microwave Heating Process," *Engineered Science*, vol. 26, p. 970, 2023.

35. W. Preechaphonkul and P. Rattanadecho, "The effects of dielectric & thermal property functions on the thermal response during the focused microwave ablation treatment in the liver cancer model: numerical investigation," Engineered Science, 2022.

36. N. Makul and G. Suaiam, "New insights into the early age time dependent dielectric evolution of pozzolan modified eco efficient cement pastes within a frequency range of 200 MHz to 6500 MHz: Experiments and statistical modeling," *Engineered Science*, 2024. doi: 10.30919/es1170.

37. S. Supasin, C. Kantala, and P. Intra, "Investigating the effect of pulsed electric field parameters on the quality of processed mango pickling," *Engineered Science*, 2024. doi: 10.30919/es1090.

# Figures

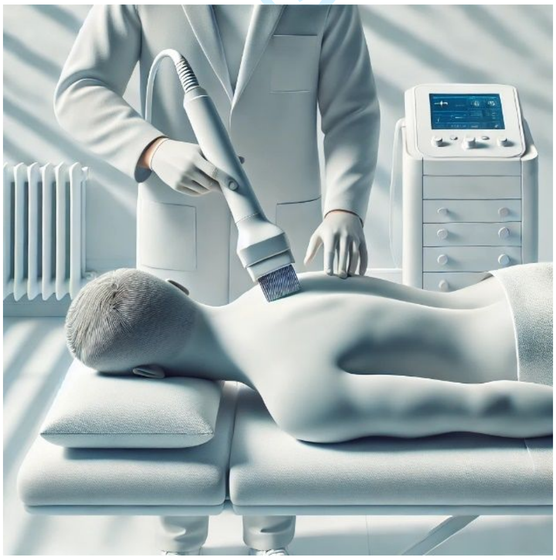

**Figure 1** The physical characteristics of ultrasound therapy used for the treatment of muscle pain and tissue recovery in patients. This includes applications aimed at alleviating discomfort caused by repetitive strain injuries or conditions such as office syndrome.

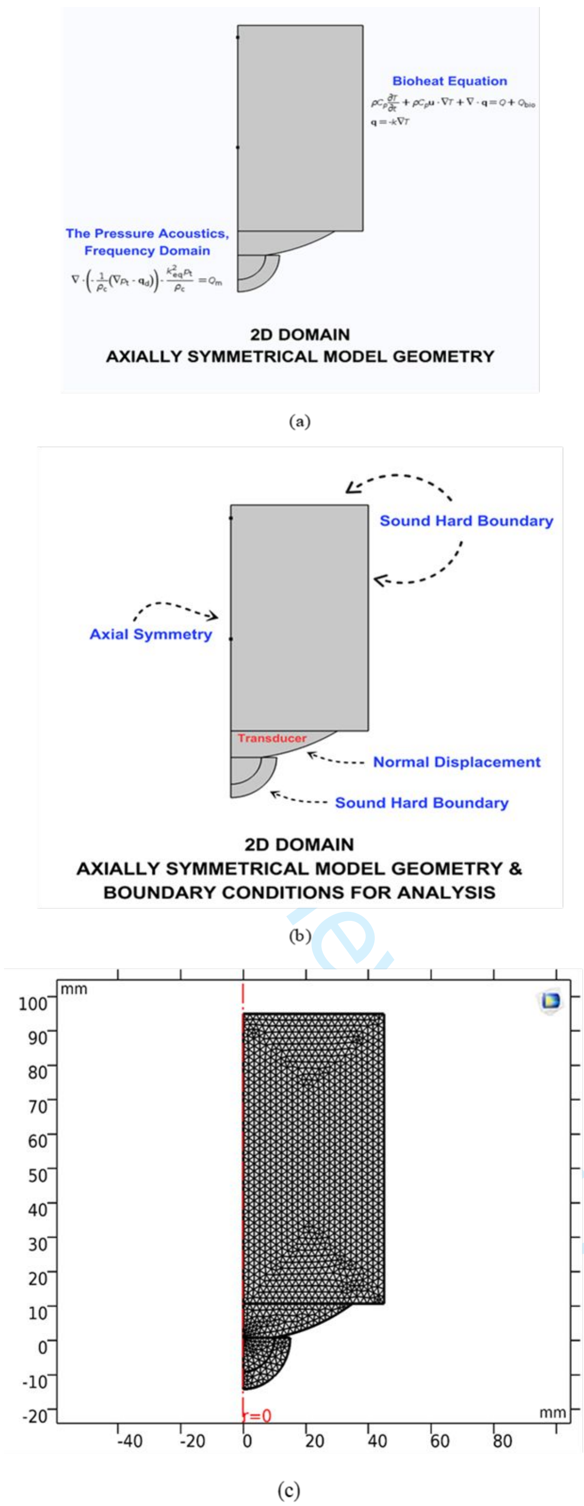


**Figure 2** The modeling framework used in the study (a) The inverted geometry and fundamental equations for simulating heat dispersion in biological tissues. (b) The inverted geometry model depicting the imposed boundary conditions. (c) The inverted geometry model illustrates the dimensions and quantity of elements included in the simulation using COMSOL Multiphysics software.

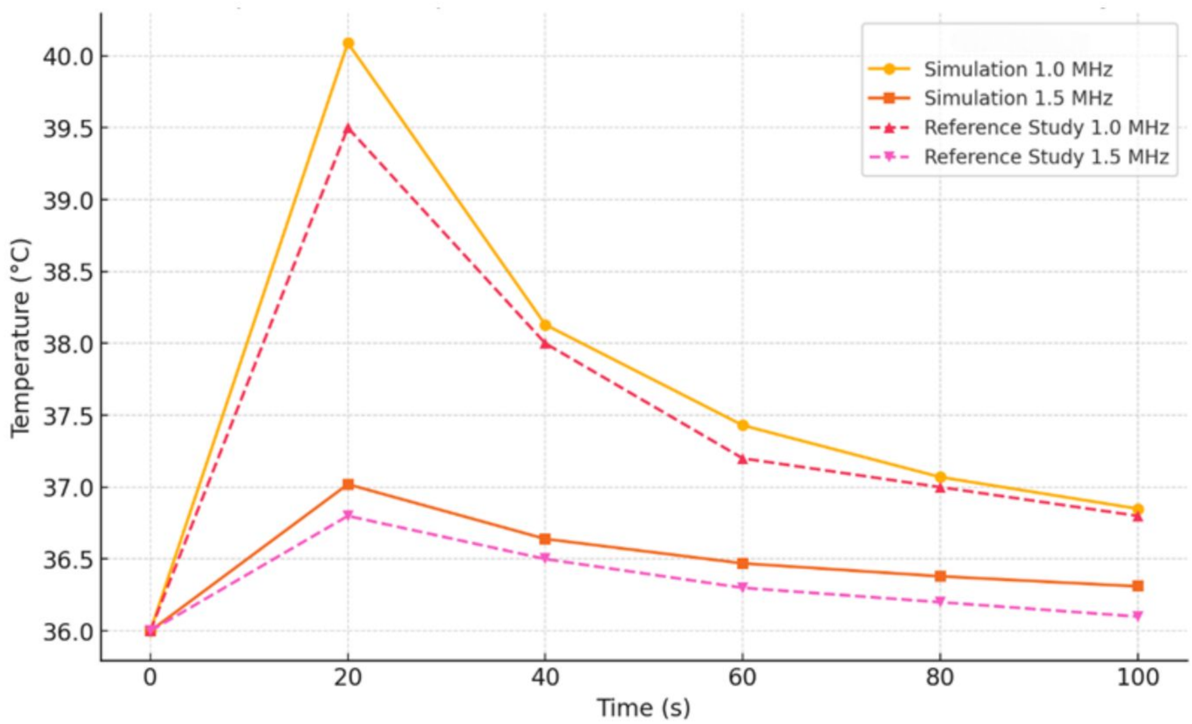


797

798

799 **Figure 3** The validation of the current model by comparing its results with previous studies
800 conducted by Leonard, J., & Merrick, M. (2004), Burr, P. O., Demchak, T. J., & Cordova, M.
801 L. (2004), and Reher, P., Doan, N., Bradnock, B., & Meghji, S. (1998).

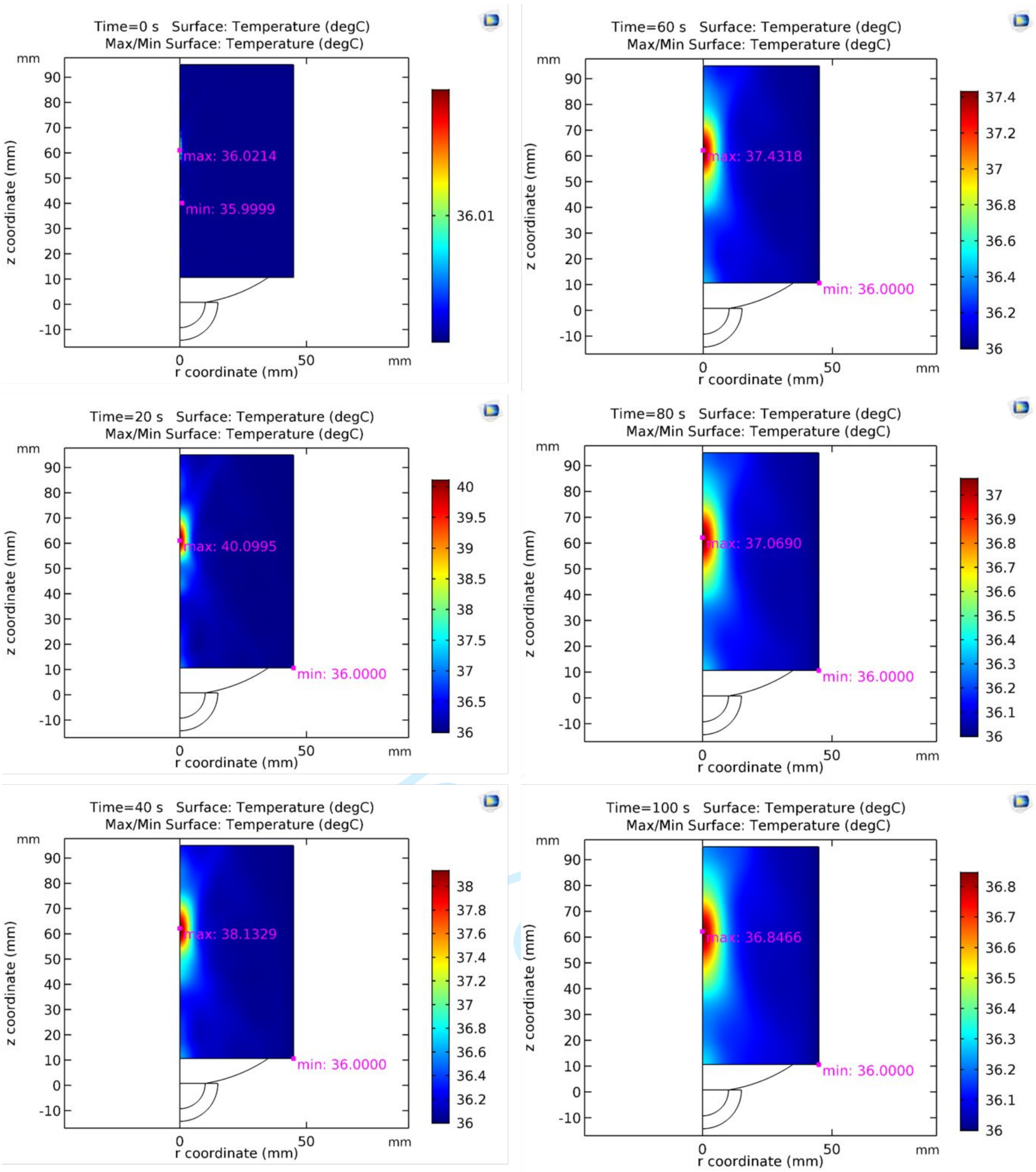


**Figure 4** The temperature distribution (°C) for ultrasound at a frequency of 1.0 MHz at time intervals of 0, 20, 40, 60, 80, and 100 seconds.

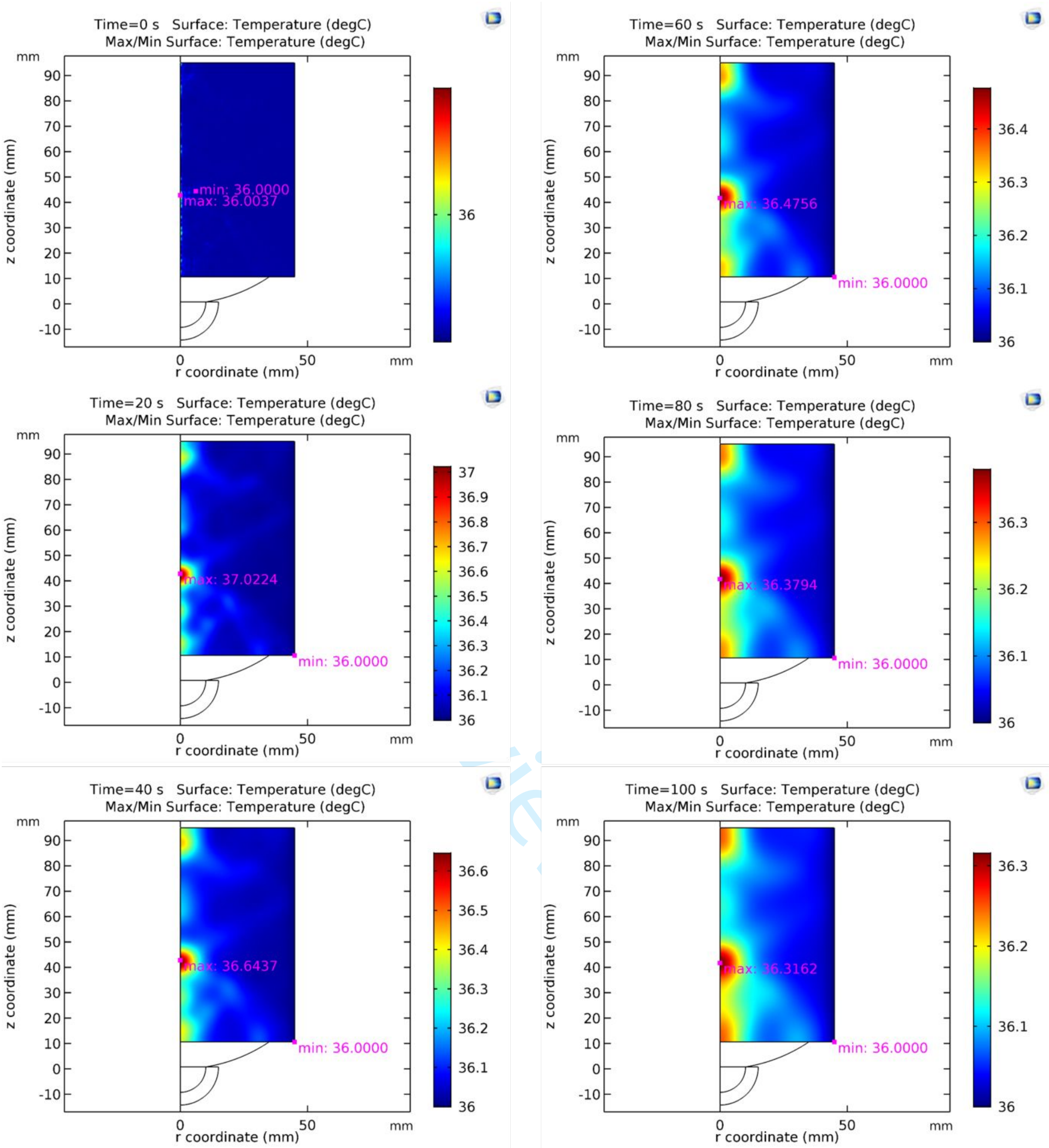


**Figure 5** The temperature distribution (°C) for ultrasound at a frequency of 1.5 MHz at time intervals of 0, 20, 40, 60, 80, and 100 seconds.

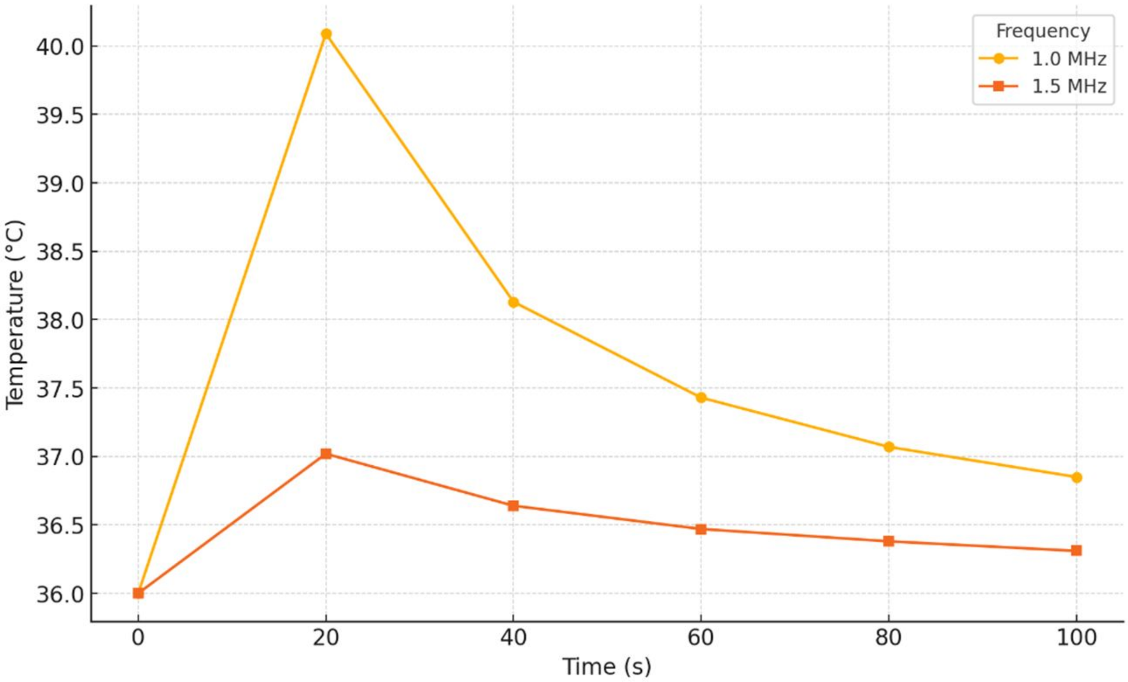


**Figure 6** The relationship between time (x-axis) and maximum temperature (y-axis) as derived from simulations at ultrasound frequencies of 1.0 MHz and 1.5 MHz.

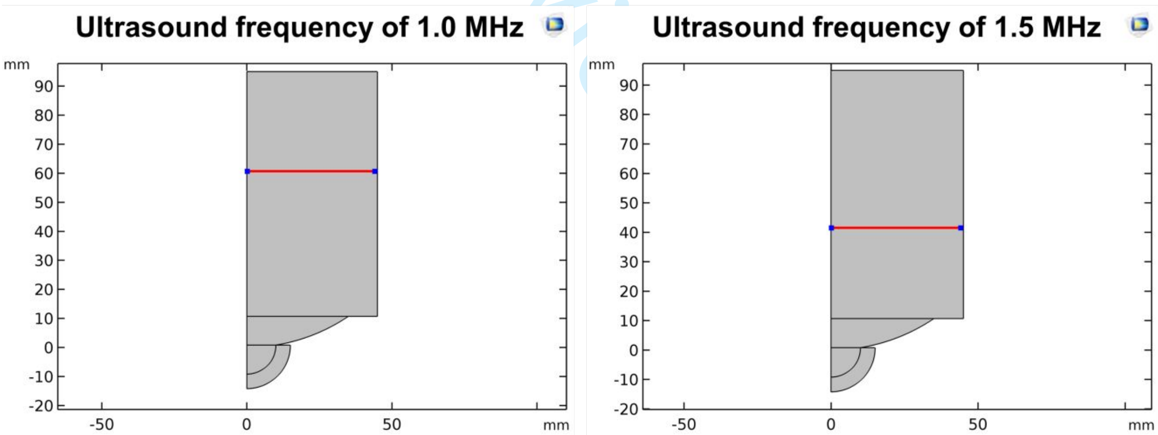


**Figure 7** The red cut line defined in specific areas in the 2D simulation space is shown to study the temperature changes in **Figure 8**.

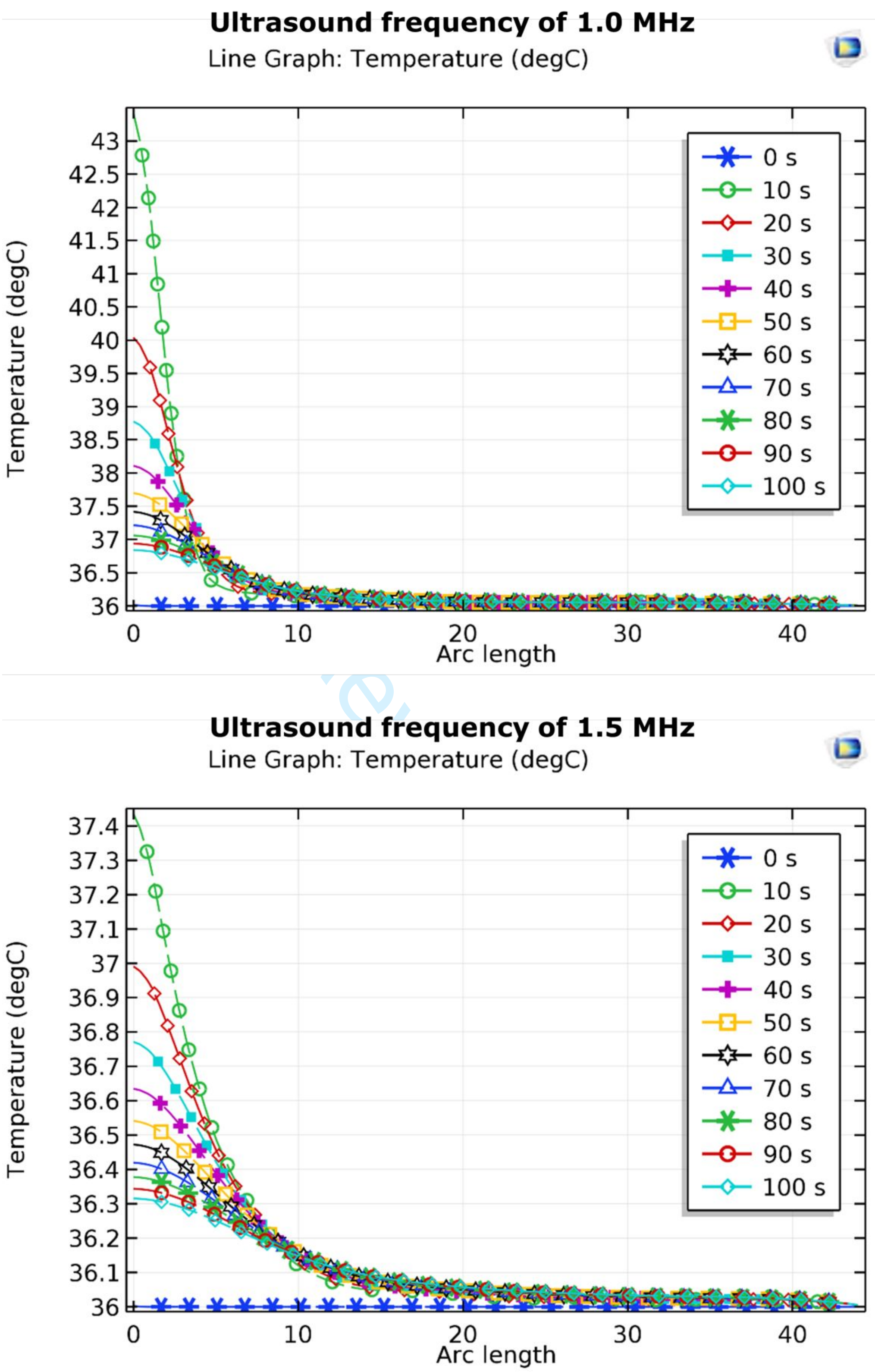


**Figure 8** Temperature distribution along the arc length of tissue under difference ultrasound frequency at different time intervals (0-100 s)

818

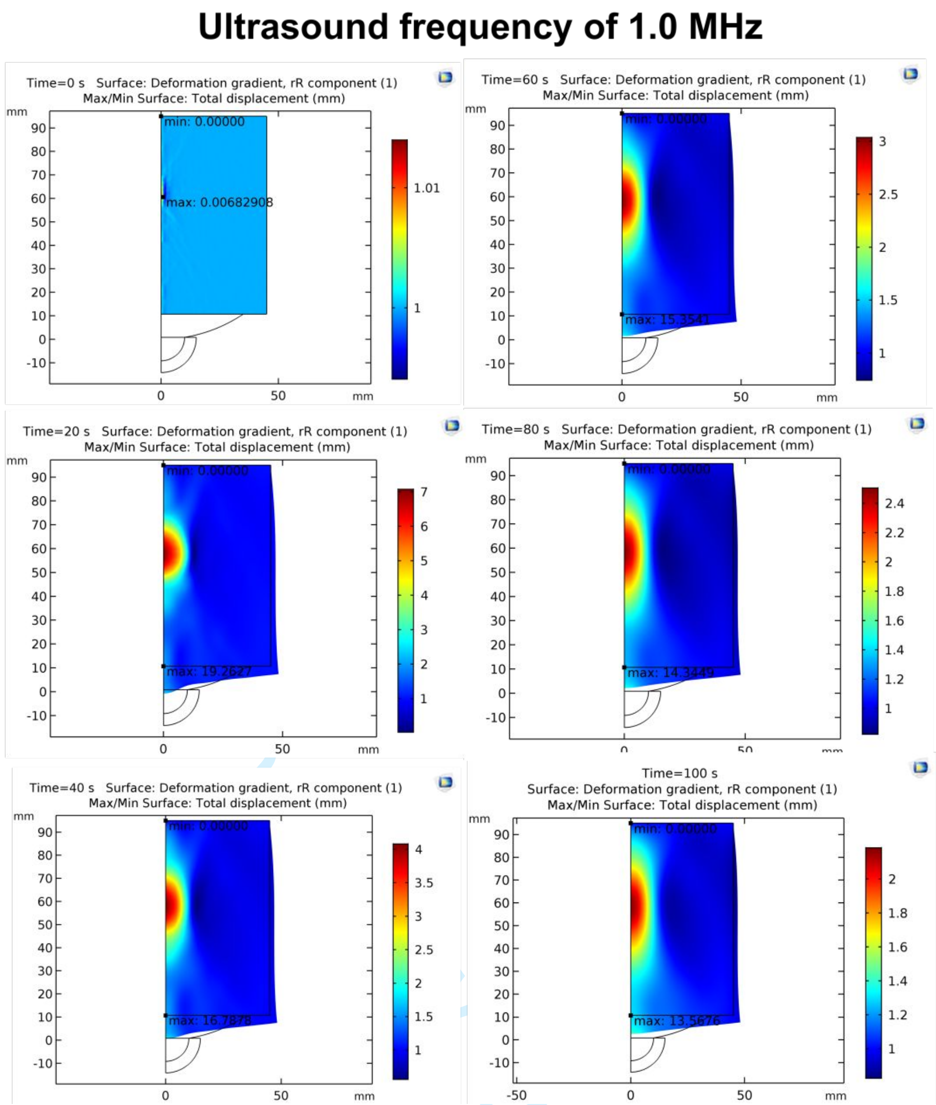


819 **Figure 9** The temporal evolution of total displacement in muscle tissue during ultrasound
820 therapy at 1.0 MHz

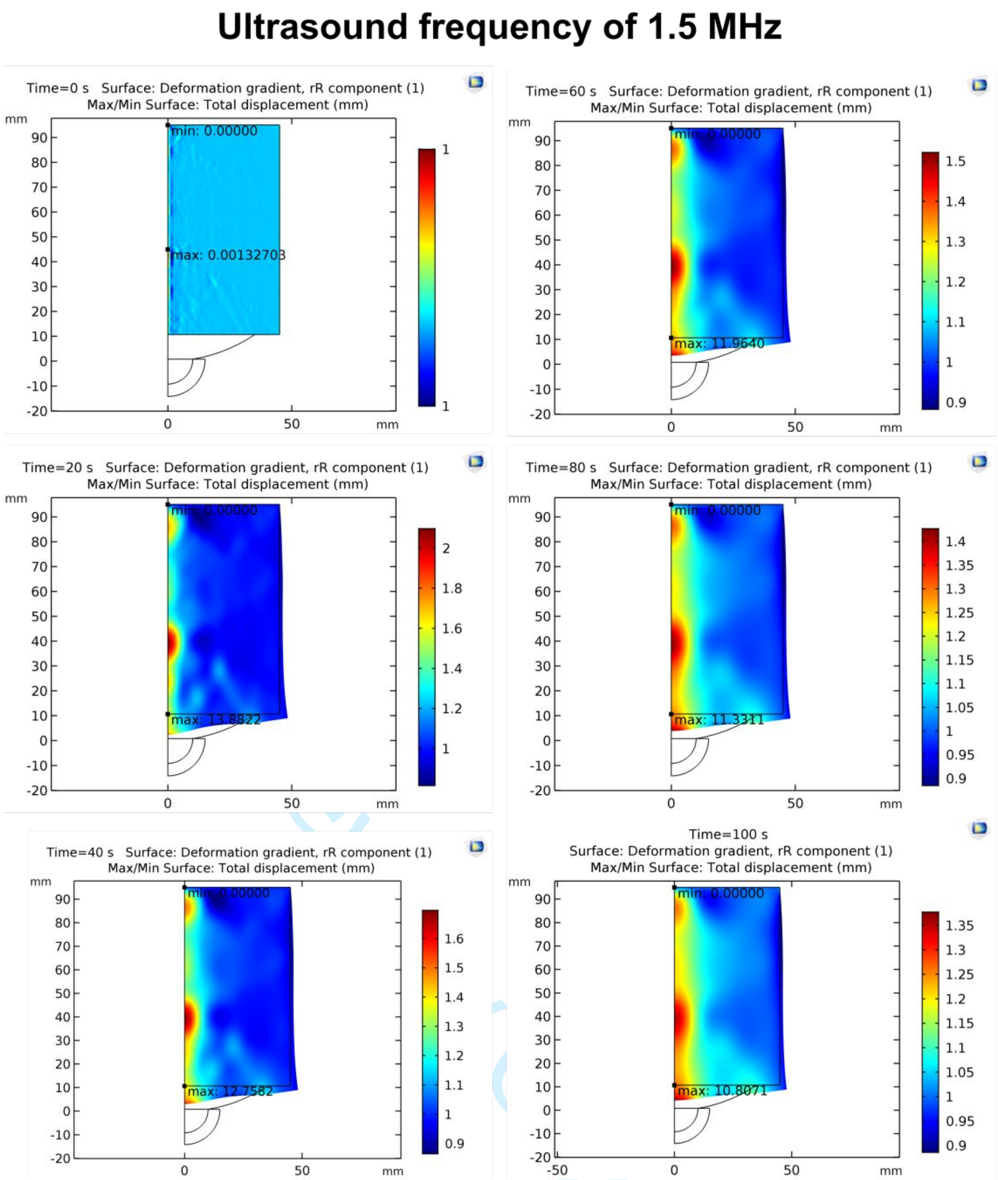


**Figure 10** The temporal evolution of total displacement in muscle tissue during ultrasound therapy at 1.5 MHz

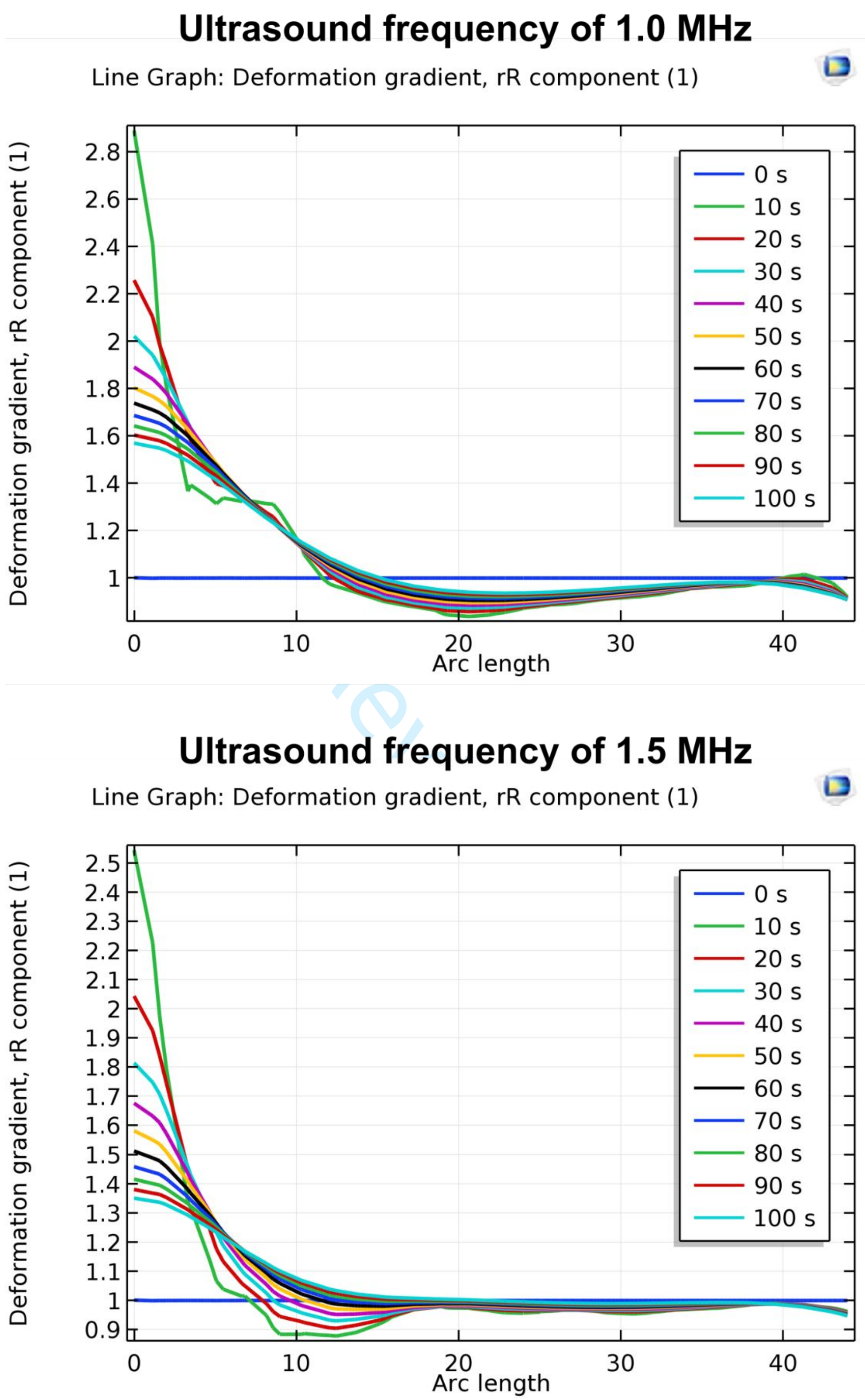


**Figure 11** The temporal evolution of the deformation gradient (rR component) in muscle tissue during ultrasound exposure at 1.0 and 1.5 MHz, respectively.

# Table

**Table1 The thermal properties and acoustic properties of tissues [13].**

| Tissue | h | c | k | ρ | $\omega_b$ | $Q_{met}$ | $c_c$ (speed of sound) | α at 1 MHz | α at 1.5 MHz | η |
|---|---|---|---|---|---|---|---|---|---|---|
| Muscle | 15 | 3800 | 0.48 | 1085 | $5.3908 \times 10^{-4}$ | 700 | 1545 ± 5 | 1.09 | 1.2819 | 1.4 |
| Blood | — | 4200 | 0.501 | 1060 | — | — | 1540 | 0.1303 | 0.1532 | 1.4 |

## Table of Contents Entry

A computational that combines acoustic, mechanical, and thermal modeling is studied to examine ultrasound-induced tissue deformation. The model demonstrates frequency-dependent effects (1.0–1.5 MHz) on stress distribution and thermal production in muscle tissue—elements frequently overlooked in prior research. This study enhances the development of safer, non-invasive therapeutic ultrasound techniques for the management of muscle discomfort.

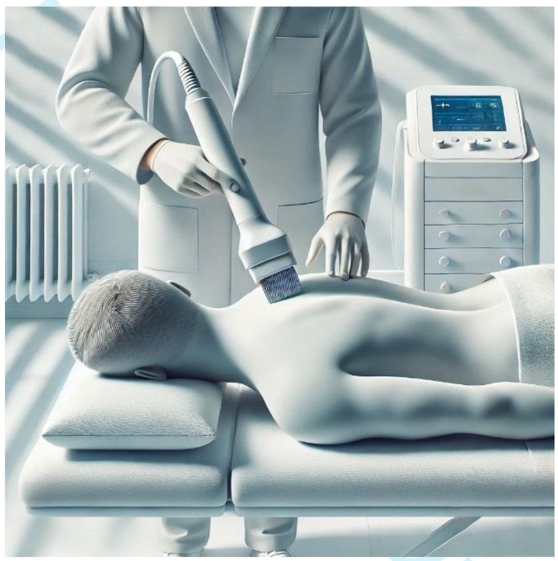

**Ultrasound frequency of 1.0 MHz**

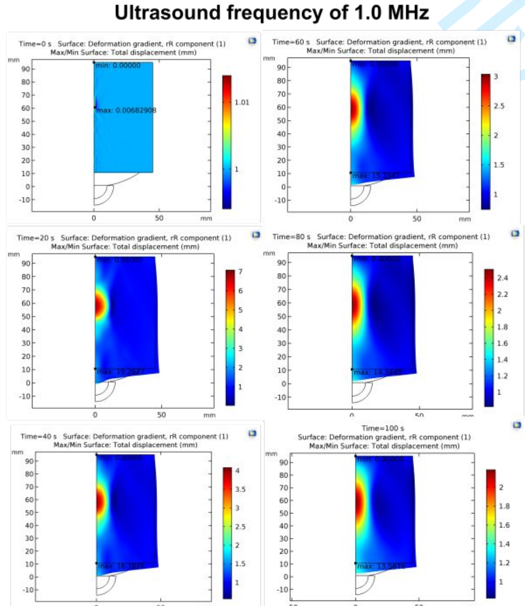

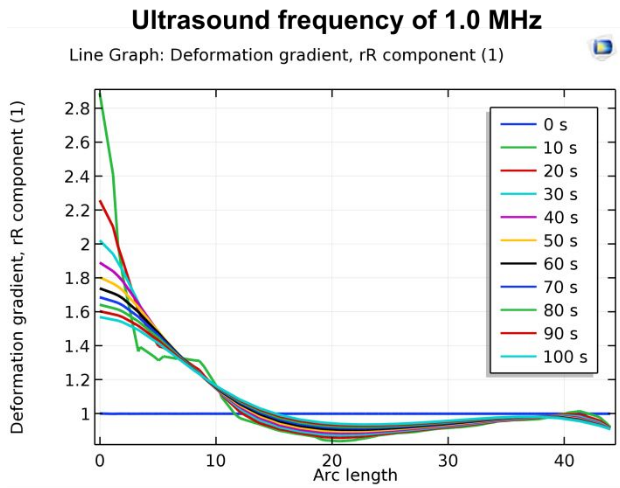
Ultrasound frequency of 1.0 MHz
Line Graph: Deformation gradient, rR component (1)
Deformation gradient, rR component (1)
Arc length
0 s
10 s
20 s
30 s
40 s
50 s
60 s
70 s
80 s
90 s
100 s

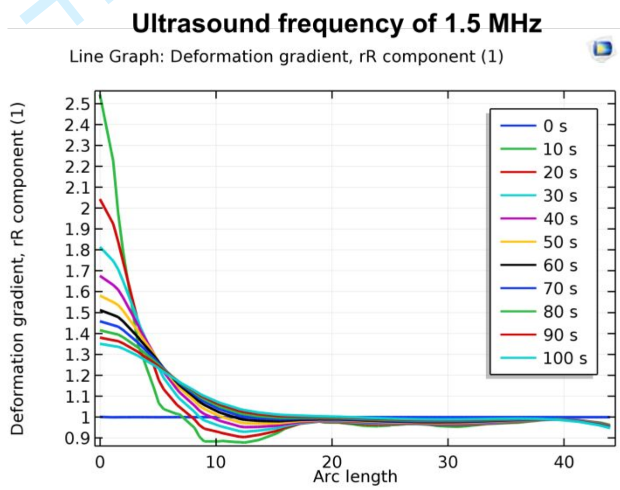
Ultrasound frequency of 1.5 MHz
Line Graph: Deformation gradient, rR component (1)
Deformation gradient, rR component (1)
Arc length
0 s
10 s
20 s
30 s
40 s
50 s
60 s
70 s
80 s
90 s
100 s

## 20-word Innovative Description

Discovering frequency-dependent biomechanical responses for customized, non-invasive therapy, this research integrates tissue deformation analysis into ultrasonic modeling.